Seasonal variation of the concentrations of nitrogenous species and their nitrogen isotopic ratios in aerosols at Gosan, Jeju Island: Implications for atmospheric processing and source changes of aerosols

Shuvashish Kundu,[1,2] Kimitaka Kawamura,[1] and Meehye Lee[3]

Received 2 October 2009; revised 25 May 2010; accepted 7 June 2010; published 20 October 2010.

[1] Atmospheric aerosol samples (n = 84) were collected at Gosan site, Jeju Island, South Korea between April 2003 and April 2004 for the measurements of total nitrogen (TN) and its isotopic ratio (δ^{15}N) as well as nitrogen species (NH_4^+ and NO_3^-). Measurements were also conducted for remained nitrogen (remained N) and removed nitrogen (removed N) on HCl fume treatment. A pronounced seasonal variation was found in the δ^{15}N of TN, remained N (mostly NH_4^+), and removed N (mostly NO_3^-). The highest mean δ^{15}N values of TN (+16.9‰ ± 4.5‰) and remained N (+20.2‰ ± 5.2‰) are detected in summer (June–August) whereas the lowest mean δ^{15}N values (+12.9‰ ± 3.4‰ and +11.3‰ ± 5.1‰, respectively) are in winter (December–February). These trends can partly be explained by an enhanced contribution of ^{15}N-enriched emissions from agricultural straw burning in China in a harvest season (summer and autumn). The mean δ^{15}N of removed N showed an opposite trend: the lowest (+8.9‰ ± 3.7‰) in warm season (March–August) and the highest (+14.1‰ ± 3.7‰) in cold season (September–February). These results can be explained by changes in source regions and emission strengths of nitrogenous species, as well as difference in secondary aerosol nitrogen formation between warm and cold seasons. Higher ratios of Ca^{2+}/Na^+ and the lowest ratios of $Na^+/(Cl^- + NO_3^-)$ are associated with lower δ^{15}N values of removed N as a result of less isotopic enrichment ($\varepsilon_{product\text{-}reactant}$) during the reaction between HNO_3 and dust particles. This study proposes that $^{15}N/^{14}N$ ratio can be regarded as process tracer of nitrogenous species in the atmosphere.

Citation: Kundu, S., K. Kawamura, and M. Lee (2010), Seasonal variation of the concentrations of nitrogenous species and their nitrogen isotopic ratios in aerosols at Gosan, Jeju Island: Implications for atmospheric processing and source changes of aerosols, *J. Geophys. Res.*, *115*, D20305, doi:10.1029/2009JD013323.

1. Introduction

[2] Although the use of nitrogen isotopic composition to understand the sources of nitrogenous species (NO_x, NH_4^+, and NO_3^-) in the atmosphere is well documented [*Hoering*, 1957; *Moore*, 1974, 1977; *Heaton*, 1986, 1987; *Freyer*, 1978a, 1991; *Pichlmayer et al.*, 1998; *Russell et al.*, 1998; *Wagenbach et al.*, 1998; *Yeatman et al.*, 2001b; *Gao*, 2002; *Martinelli et al.*, 2002; *Xiao and Liu*, 2002; *Hastings et al.*, 2003; *Kawamura et al.*, 2004; *Savarino et al.*, 2007; *Widory*, 2007], its usefulness has not well been explained in terms of the complex atmospheric processing and mechanisms [*Freyer et al.*, 1993; *Yeatman et al.*, 2001c; *Widory*, 2007].

[3] Nitrate is the ultimate product of atmospheric oxidation of NO_x (NO and NO_2), which is produced in daytime via

$$NO + O_3 \rightarrow NO_2 + O_2, \quad (1)$$

$$NO_2 + h\nu \rightarrow NO + O, \quad (2)$$

$$O + O_2 \rightarrow O_3, \quad (3)$$

$$NO_2 + OH \rightarrow HNO_3, \quad (4)$$

and in nighttime via

$$NO_2 + O_3 \rightarrow NO_3 + O_2, \quad (5)$$

$$NO_3 + NO_2 \rightarrow N_2O_5, \quad (6)$$

$$N_2O_5 + H_2O \rightarrow 2HNO_3. \quad (7)$$

[1]Institute of Low Temperature Science, Hokkaido University, Sapporo, Japan.
[2]Graduate School of Environmental Science, Hokkaido University, Sapporo, Japan.
[3]Department of Earth and Environmental Sciences, Korea University, Seoul, South Korea.

0148-0227/10/2009JD013323

[4] The incorporation of HNO_3 to aerosols via heterogeneous or homogeneous reactions varies between the locations [*Wolff*, 1984]. HNO_3 competes to react with sea salt, dust aerosol and NH_3 via

$$HNO_3 + NaCl \rightarrow NaNO_3 + HCl, \quad (8)$$

$$2HNO_3 + CaCO_3 \rightarrow Ca(NO_3)_2 + CO_2 + H_2O, \quad (9)$$

$$HNO_3 + NH_3 \rightarrow NH_4NO_3. \quad (10)$$

[5] Nonvolatile aerosol nitrogen on coarse mode is produced from reactions (8) and (9), whereas semivolatile aerosol nitrogen on fine mode is produced from reaction (10). NH_4NO_3 can dissociate [*Allen et al.*, 1989] and regenerate HNO_3, which is dependent upon a number of variables including temperature, relative humidity, aerosol size, and the extent of internal mixing within aerosols [*Harrison and MacKenzie*, 1990; *Meng and Seinfeld*, 1996; *Clegg et al.*, 1998]. HNO_3 regenerated from the dissociation process can react with sea salt and dust particles [*Brimblecombe and Clegg*, 1988; *Pakkanen*, 1996; *Zhuang et al.*, 1999; *Spokes et al.*, 2000; *Yeatman et al.*, 2001a]. NH_3 also reacts irreversibly with H_2SO_4 to produce $(NH_4)_2SO_4$ and NH_4HSO_4 in the fine mode [*Ottley and Harrison*, 1992]. Additionally, there is evidence for dissolution/coagulation processes that shift both NH_4^+ and NO_3^- to the coarse mode [*Ottley and Harrison*, 1992; *Yeatman et al.*, 2001a].

[6] Nitrogen compounds play key roles in the formation of smog, aerosol, and ozone and in the determination of acidity in precipitation [*Marsh*, 1978; *Galloway and Likens*, 1981]. Possible shift of NO_3^- and NH_4^+ to the coarse mode significantly enhances the rate of nitrogen deposition to the coastal ecosystems and hence marine productivity [*Galloway et al.*, 1995; *Jickells*, 1998; *Spokes et al.*, 2000; *Duce et al.*, 2008]. It is therefore very important to know atmospheric processing of nitrogenous species as discussed earlier and their sources in the atmosphere.

[7] The present research has been conducted with the aim of evaluating the usefulness of $^{15}N/^{14}N$ ratio to interpret the complex atmospheric processing and sources of nitrogen species in the East Asian aerosols collected at Gosan site in Jeju Island, the East China Sea, for 1 year from 2003 to 2004. Here we present seasonal variations of $\delta^{15}N$ of total nitrogen (TN), remained nitrogen (mostly composed of NH_4^+), and removed nitrogen (mostly composed of NO_3^-) in the aerosol samples. Then, we interpret the observed isotopic composition ($\delta^{15}N$) and its seasonal variations based on the chemistry of nitrogenous species in the atmosphere and air mass transport pathways with which we can backtrack their source regions. Although $\delta^{15}N$ data have been reported previously as part of comprehensive study of organic and inorganic chemistry of Gosan aerosols [*Kawamura et al.*, 2004], the present paper focuses on $\delta^{15}N$ composition of nitrogenous species and discuss in more details on the chemical processes that govern the seasonal variations of the $\delta^{15}N$ values in aerosols.

2. Methods

2.1. Site Description

[8] Gosan site is located on a cliff (~71 m ASL) at the western tip of Jeju Island (33°29′N, 126°16′E). It is approximately 100 km off the south of Korean Peninsula, ~500 km off the east of China (Jiangsu province or Shanghai), ~200 km off the west of Kyushu Island, Japan, and ~1000 km off the northeast of Taiwan (Figure 1). The site and its surroundings are covered with grasses but no trees. Because of its location and very limited local anthropogenic emissions [*Kim et al.*, 1998], Gosan has been considered as an ideal site to monitor the impact on air quality of the western rim of the North Pacific due to the outflows from East Asia [*Carmichael et al.*, 1996, 1997; *Chen et al.*, 1997]. Gosan was used as a supersite of ACE-Asia campaign in 2001 [*Huebert et al.*, 2003], and PEM-West A and PEM-West B programs conducted between 1991 and 1994 [*Hoell et al.*, 1996, 1997]. It is now used as one of superstations of Atmospheric Brown Cloud (ABC) program [*Lee et al.*, 2007]. More detailed description of this site is given elsewhere [*Kim et al.*, 1998; *Kawamura et al.*, 2004; *Lee et al.*, 2007].

2.2. Aerosol Sampling

[9] Total suspended particles (TSP) in the atmosphere were collected at Gosan site over 2–7 days throughout the year from 2003 April to 2004 April. TSP samples (n = 84) were collected on precombusted quartz fiber filters using a high volume air sampler (Kimoto AS-810) installed on the roof of a trailer house (~3 m above the ground). Before and after the sampling, filters were put in clean glass jars (150 mL) with Teflon-lined screw cap. Samples were transported to our laboratory in Sapporo and stored in a dark freezer room at −20°C until analysis. Field blank filters were collected every month.

2.3. Analytical Methods

[10] In the present study, we follow a simple approach to approximate the nitrogen isotopic composition of both NH_4^+ and NO_3^- [*Kawamura et al.*, 2004]. We expose the filter cuts of samples to HCl fuming in a desiccator in order to remove NO_3^-. On the basis of the ion chromatographic (IC) analyses of the samples before and after HCl treatment, we confirm that NO_3^- is completely removed, but NH_4^+ remains intact. Here we refer nitrogen that remained on the filters due to HCl fume treatment as remained nitrogen (remained N) whereas nitrogen flew away from the filters as removed nitrogen (removed N). Quality assurance of this procedure will be given later with evidence to prove that remained N is mainly composed of NH_4^+ whereas removed N is mainly composed of NO_3^-.

[11] For TN and remained N analyses, two small discs (area 2.54 cm^2) were cut off from each filter sample. One disc was put in a tin cup and shaped into a rounded ball using a pair of flat-tipped tweezers. The samples were introduced into the elemental analyzer (EA; model: NA 1500 NCS, Carlo Erba Instruments) using an autosampler

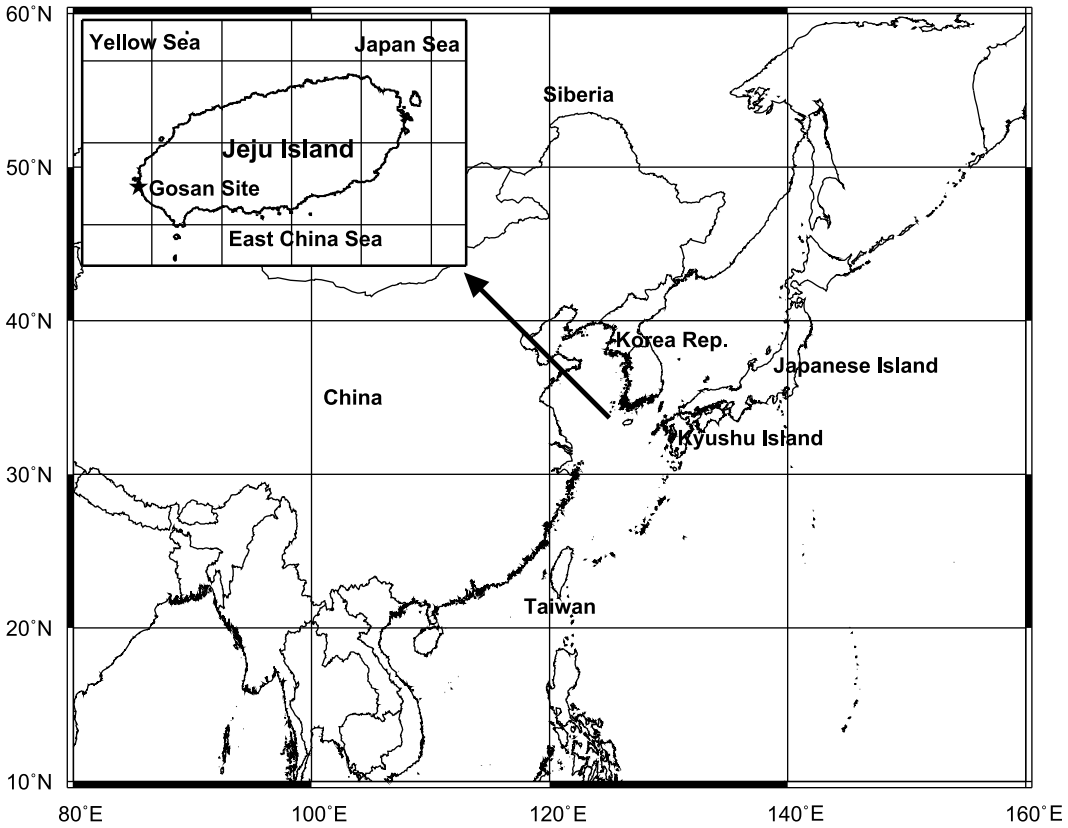

Figure 1. Map showing the geographical region where our sampling was carried out. Inset shows location of Gosan site (marked with asterisk) in the west coast of Jeju Island, South Korea. The island is surrounded by the oceans in all directions.

and were oxidized in a combustion column packed with chromium trioxide at 1020°C, in which the tin container burns (>1400°C) to promote the intensive oxidation of sample materials in an atmosphere of pure oxygen. The combustion products are transferred to a reduction column packed with metallic copper that was maintained at 650°C. Here excess oxygen is removed and nitrogen oxides coming from the combustion tube are reduced to molecular nitrogen (N_2). The N_2 was isolated from CO_2 online using a gas chromatograph (GC) installed in EA and then measured with a thermal conductivity detector. Aliquots of N_2 gas were then introduced into an isotope ratio mass spectrometer (ThermoQuest, Delta Plus) through a ConFlo II interface (ThermoQuest) to monitor $^{15}N/^{14}N$ ratios. The nitrogen isotopic composition was calculated using the following standard isotopic conversion equation.

$$\delta^{15}\mathrm{N} = \left[\frac{\left(^{15}\mathrm{N}/^{14}\mathrm{N}\right)_{\mathrm{sample}}}{\left(^{15}\mathrm{N}/^{14}\mathrm{N}\right)_{\mathrm{standard}}} - 1 \right] \times 1000$$

[12] An external standard (acetanilide) was used to determine TN, remained N and their isotopic ratios. The $\delta^{15}N$ value of acetanilide is 11.89‰.

[13] Another disc was placed in a 10 mL glass vial and exposed to fuming HCl overnight in a glass desiccator (40 cm wide) to remove NO_3^-, which facilitates only the measurement of remained N (mostly NH_4^+) on the filter sample and its nitrogen isotopic composition. Similar analytical procedure has been used in the previous study [*Kawamura et al.*, 2004], in which the $\delta^{15}N$ values of removed N were calculated using the following isotopic mass balance equation.

$$F_{\text{remained N}} + F_{\text{removed N}} = 1$$

$$F_{\text{remained N}} = \frac{\text{remained N}}{\text{TN}}, \quad F_{\text{removed N}} = \frac{\text{TN} - \text{remained N}}{\text{TN}}$$

$$\delta^{15}\mathrm{N_{TN}} = F_{\text{remained N}} \times \delta^{15}\mathrm{N_{remained\ N}} + F_{\text{removed N}} \times \delta^{15}\mathrm{N_{removed\ N}}$$

[14] "Ammonium" (remained N) and "nitrate" (removed N) were not explicitly measured but were measured using a chemical method of HCl fuming and EA. Hereafter, we use symbols NH_4^+* and NO_3^-*, which mean concentrations of remained N ("ammonium") and removed N ("nitrate"), respectively.

[15] For the analyses of water-soluble inorganic ion, aliquots (area 2.54 cm^2) of filter samples were placed in 50 mL glass vials, soaked using 10 mL of Milli Q water, and agitated over 15 min using an ultrasonicator. The extracts were filtered with prewashed Millex (Millipore Corporation, Bedford, USA, 0.45 μm) syringe filters. The concentrations of the ions in the aqueous extracts were determined using a Metrohm 761 IC (Metrohm, Herisau, Switzerland). Anions

Table 1. Determination of the $\delta^{15}N$ of Pure NH_4^+, NO_3^-, and Their Mixture With Water-Soluble Cations and Anions Spiked on Quartz Fiber Filter Disc (18 mm in Diameter) at Different Concentration Levels[a]

Species	Spiked Levels (μg)	$\delta^{15}N$ (‰) Without HCl Treatment	$\delta^{15}N$ (‰) With HCl Treatment
NH_4^+	1.3	6.9	6.8
	2.6	6.8	6.7
	5.2	6.6	7.1
NO_3^-	1.6	8.4	-
	6.4	8.2	-
	16.0	7.9	-
$NH_4^+ + NO_3^-$	1.3 + 1.6	7.5	6.7
	2.6 + 3.2	7.1	7.0
	5.2 + 6.4	7.0	6.9
$NH_4^+ + NO_3^-$	1.0 + 3.0	7.1	8.1
with cations	4.0 + 12.0	7.3	7.8
and anions	6.0 + 20.0	7.1	8.0

[a]The $\delta^{15}N$ of $NH_4^+ + NO_3^-$ in the second column is for NH_4^+ only as a result of complete removal of NO_3^- due to HCl treatment. It is confirmed that NO_3^- is completely removed and NH_4^+ remains intact due to HCl treatment by analyzing the samples before and after HCl treatment using an ion chromatography instrument.

in the aqueous extracts were separated on a Shodex SI-90 4E column with 1.8 mM Na_2CO_3 and 1.7 mM $NaHCO_3$ (Kanto Chemical, Japan) as eluent. Cations were isolated on a Shodex YK-421 column with 4 mM H_3PO_4 as eluent (Kanto Chemical, Japan). The injection loop volume was 200 μL. Cations and anions are quantified against a standard calibration curve.

2.4. Quality Assurance of Data

[16] Field blanks for TN showed very small peaks of nitrogen on GC chromatogram, which were equivalent to 0.4%–9% of real samples. The reported concentrations for both TN and NH_4^+*, and their $\delta^{15}N$ values were corrected for the field blanks. The analyses of a few samples (n = 7) were replicated for TN and NH_4^+*, and their isotopic ratios. The precisions for TN and NH_4^+* measurements ranged 1.4%–5% (av. 3%) whereas those for the $\delta^{15}N$ measurements ranged 0.03‰–0.36‰ (av. 0.23‰).

[17] In order to check whether any isotopic fractionation occurs during the exposure of filter samples to fuming HCl, we spiked different amounts of pure NH_4^+, NO_3^-, and their mixtures with other cations and anions on fresh quartz fiber filters to mimic the ionic composition of our filter samples. Then we measured nitrogen isotopic composition of the spiked samples before and after HCl fume treatment. The results are shown in Table 1. The $\delta^{15}N$ values of spiked NH_4^+ samples are 6.6‰–6.9‰ with a mean of 6.8‰ and standard deviations of ±0.1‰, which are similar to those of HCl-treated spiked NH_4^+, and NH_4^+ plus NO_3^- samples. The isotopic mass balance equation shows that the $\delta^{15}N$ values of eliminated NO_3^- from spiked NH_4^+ plus NO_3^- samples on HCl treatment are similar to those of spiked NO_3^- samples. The $\delta^{15}N$ values of spiked samples with different levels of mixture of NH_4^+, NO_3^-, and other water-soluble cations and anions are also similar. These results suggest that difference in the concentration levels of NH_4^+ and NO_3^- does not cause any isotopic fractionation during HCl fume treatment. It is also important to note that after the HCl treatment on the spiked filter samples NO_3^- peak was not detected on the ion chromatograms, indicating that NO_3^- was completely removed from the filter.

[18] Field blanks for ions showed very small peaks of NH_4^+ and NO_3^-. They were less than 0.1%–2% and 0.02%–0.6% of real samples, respectively. The concentrations of ions reported here are corrected for the field blanks. In order to examine whether 15 min ultrasonication in 10 mL water can completely extract NH_4^+ and NO_3^- ions from the filters, a few samples (n = 7) were ultrasonicated with the same amount of water for longer periods (>30 min). No significant differences in the concentrations of ions between the extraction periods were observed. A few samples (n = 7) were also subjected to replicate analyses. The coefficients of variations for NH_4^+ and NO_3^- measurements were about 2% and 6%, respectively.

[19] The nitrogen contents in NH_4^+ and NO_3^- were compared with TN measured by EA for data quality assurance. Figure 2 shows a relation in the concentrations between ($NH_4^+ + NO_3^-$)-nitrogen and TN. A very good correlation suggests that total nitrogen in our filter samples is mainly composed of NH_4^+ and NO_3^-, and nonwater soluble nitrogen (probably organic nitrogen) accounts for only 3% of TN.

[20] The exposure of aerosol samples to fuming HCl overnight removed 5%–90% of TN (av. 36%). Strong relations were also obtained between NH_4^+-N measured by IC and NH_4^+*-N measured by EA (r^2 = 0.94) and between NO_3^--N measured by IC and NO_3^-*-N measured by EA (r^2 = 0.89) with slopes close to unity and intercepts of nearly zero

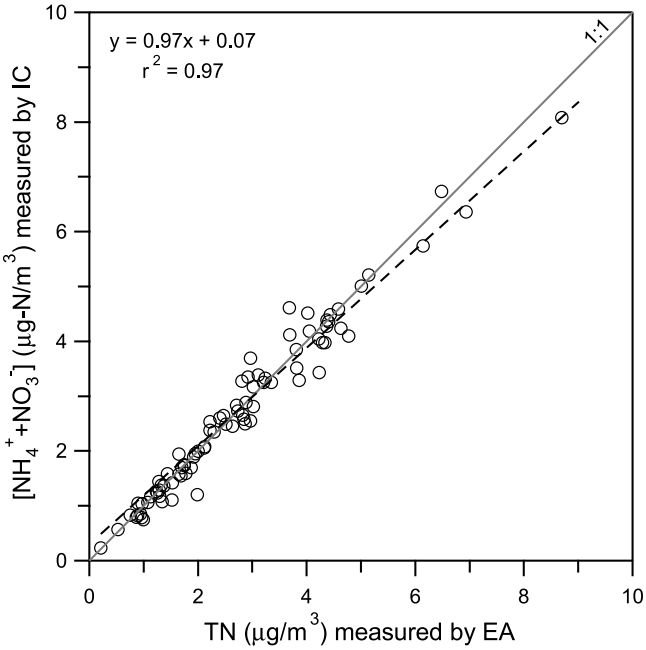

Figure 2. Relation between ammonium-plus nitrate-nitrogen (NH_4^+-N + NO_3^--N) and total nitrogen (TN) in aerosol samples from Gosan. Ammonium and nitrate ions were measured by an ion chromatography (IC) instrument, whereas TN was measured by an elemental analyzer (EA). See the text for the methods.

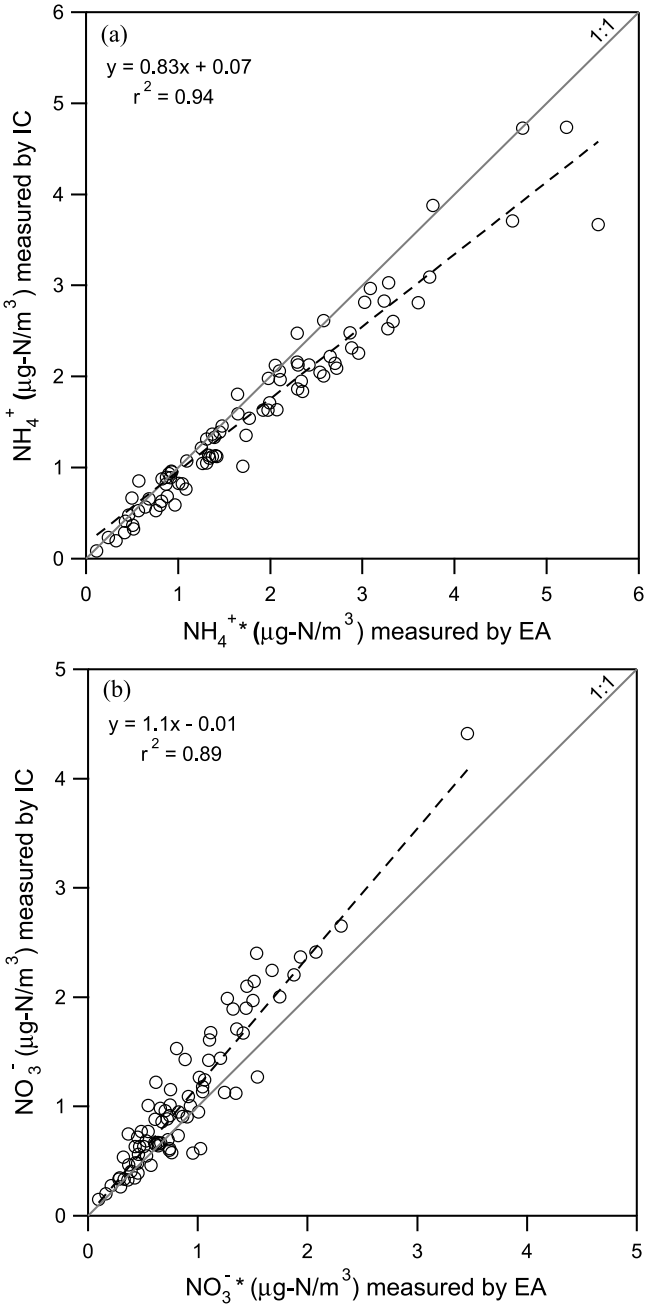

Figure 3. Relation between (a) ammonium-nitrogen (NH_4^+-N) and NH_4^+*-N and (b) nitrate-nitrogen (NO_3^--N) and NO_3^-*-N. NH_4^+*-N was measured by an elemental analyzer (EA) after the exposure of aerosol samples in fuming HCl over night, whereas NO_3^-*-N was calculated by deducting NH_4^+*-N from total nitrogen (TN). See the text for methods.

(Figures 3a and 3b). On the basis of these observations, we can postulate that NH_4^+*-N measured by EA is mainly composed of NH_4^+ whereas NO_3^-*-N measured by EA is mainly composed of NO_3^-. Similar hypothesis was given by *Kawamura et al.* [2004]. In order to prove this hypothesis, we analyzed a number of samples (n = 10) for the determination of NH_4^+ and NO_3^- using the IC technique before and after HCl fume treatment. We found that HCl fume treatment completely removed NO_3^-, but the concentration of NH_4^+ remained almost unchanged (<5%). These results confirm that the above hypothesis is correct.

2.5. Potential Sampling Artifacts Associated With Quartz Fiber Filter

[21] Aerosol samples collected on quartz fiber filters may have two types of sampling artifacts: (1) adsorption of gaseous HNO_3 and NH_3 onto aerosols already collected within the sampler or onto the collection substrate [*McMurray*, 2000] and (2) dissociation of NH_4^+ salts such as NH_4NO_3 on the filter [*Zhang and McMurray*, 1992]. Simultaneous measurements of NH_4^+ and NO_3^- in aerosols, and their gaseous precursors (NH_3 and HNO_3, respectively) can provide the quantitative estimation of the first type of artifacts. This type of measurements is not available for our study. However, we can estimate this artifact based on the previous studies carried out at our sampling site. *Kim and Seinfeld* [1995] reported that the ratio of particulate NO_3^- to total nitrate (gaseous HNO_3 + particulate NO_3^-) was 0.82 in spring whereas the annual mean of particulate NO_3^- fraction at Gosan site was 0.74 with ±0.1 deviations for the majority of months [*Hayami and Carmichael*, 1998]. Their gas-aerosol equilibrium model observations suggest a strong tendency for HNO_3 to preferentially exist in the aerosol phase. *Harrison and Pio* [1983] observed that the adsorption of NH_3 onto marine aerosols collected on the filter substrate was insignificant.

[22] Analysis of aerosol composition data measured at Gosan site from March 1992 to December 1994 using a gas-aerosol equilibrium model suggests that particulate NO_3^- and Cl^- are mostly present in the coarse mode and NH_4^+ is in the fine mode to neutralize nss-sulfate [*Hayami and Carmichael*, 1997], being consistent with the size distribution of these species in aerosols collected on Teflon substrate from the same site during Asian dust and nondust storm events [*Park et al.*, 2004]. This provides little formation of NH_4NO_3 and NH_4Cl. On the other hand, we found a good correlation (r^2 = 0.81) between NH_4^+ and SO_4^{2-} in the aerosol samples studied here. The annual mean molar ratio of NH_4^+/SO_4^{2-} was calculated as 1.1 with ±0.3 deviations. These results indicate a close association of NH_4^+ with SO_4^{2-}, suggesting that the second artifact (e.g., dissociation of NH_4NO_3 on the filter) should not be important in our study. We therefore conclude that the presence of coarse mode NO_3^- and NH_4^+ collected on the quartz fiber filters cannot be explained by a sampling artifact and thus the reported concentrations and isotopic ratios of nitrogenous species are real.

2.6. Cluster Analysis of Air Mass Backward Trajectories (April 2003 to April 2004)

[23] Three-dimensional 5 days-air mass backward trajectories arriving at Gosan were calculated with Hybrid Single-Particle Lagrangian Integrated Trajectory (HYSPLIT) model [*Draxler et al.*, 2006] using FNL meteorological data of NOAA/ARL (National Oceanic and Atmospheric Administration/Air Resources Laboratory). The backward trajectories were calculated four times a day at 0000, 6000, 1200, and 1800 UTC. We collected aerosol samples for 335 days from April 2003 to April 2004. Samples could not be collected for the other remaining days due to either technical failure of our sampler or adverse meteorological conditions. Aerosol samples were collected for 117 days in spring (n =

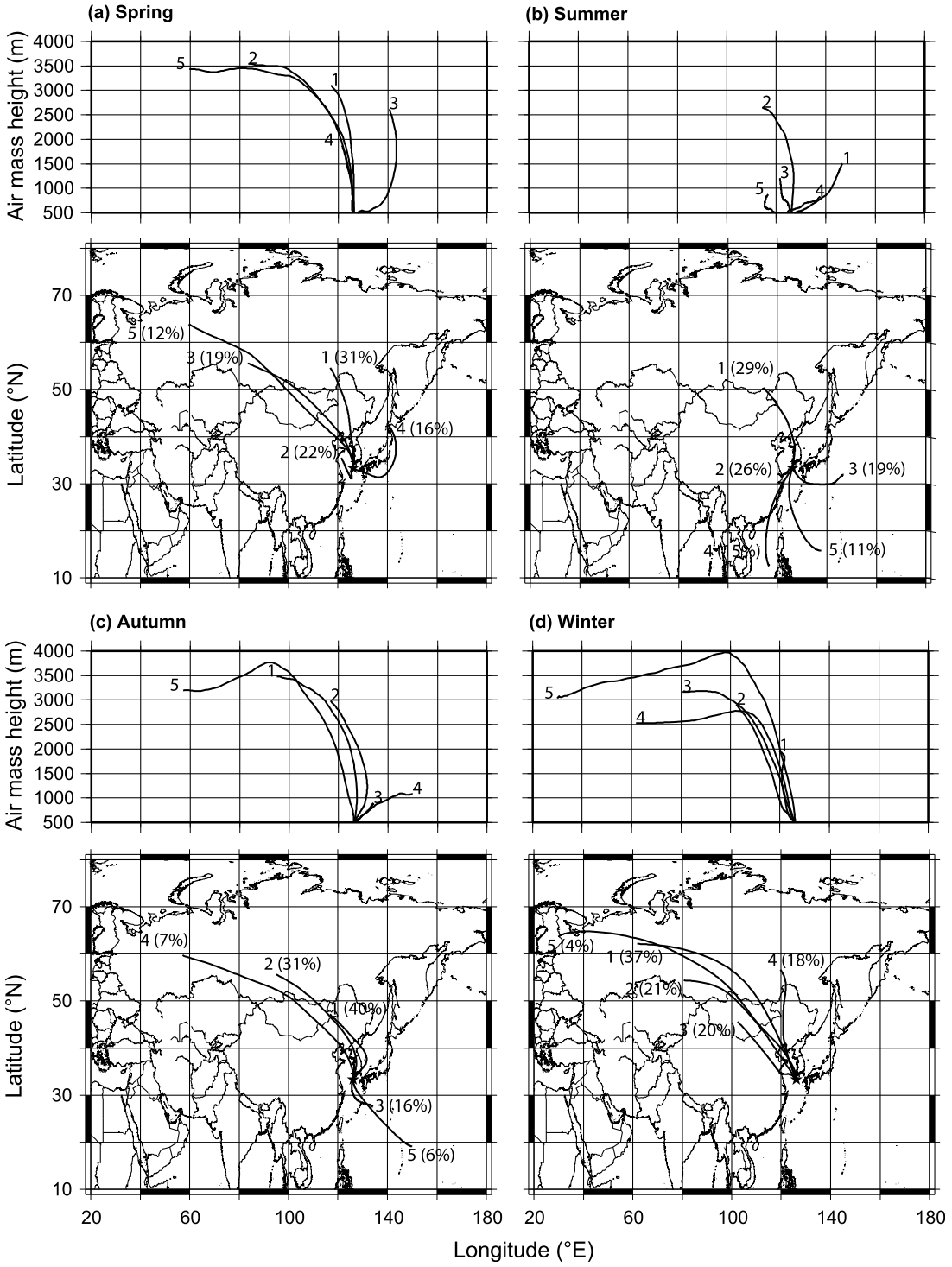

Figure 4. Mean vertical and horizontal plots of three dimensional air mass backward trajectories for the main trajectory clusters in (a) spring (March–May), (b) summer (June–August), (c) autumn (September–November), and (d) winter (December–February). Five days backward trajectories at 500 m agl were drawn with the NOAA HYSPLIT model using FNL data of NOAA/ARL. The trajectories in each season were grouped into five clusters as suggested by the model. The numbers 1–5 indicate the name of mean clusters. Clusters are arbitrarily named according to descending order of the origin of air mass transport. The numbers in brackets indicate the percentage of total air mass transport from the origins. The asterisk indicates the location of sampling site. See the text for cluster analysis and Table 2 for detailed description of the pathways of mean trajectories for each cluster.

Table 2. Summary of the Origins and Pathways of the Mean Backward Air Mass Trajectories for Different Seasons Shown in Figure 4[a]

Season	Name of Mean Trajectory	Origin of Air Masses	Description of Trajectory Pathways			Comments
			Trajectory Path 1	Trajectory Path 2	Trajectory Path 3	
Spring	1	Southern Siberia	Inner Mongolia[b]	Liaoning[c]	Eastern side of South Korea	All of the air masses are originated from either inland of East Asia or Siberian plateau of Russia. It is to be noted that a significant time (22%) in this season Gosan site remains under the influence of heavily polluted air masses (mean trajectory 2, slow moving air mass).
	2	Shangdong[c]	Yellow Sea			
	3	Western Siberia	Mongolia	Inner Mongolia[c]	Liaoning[c]	
	4	Hokkaido Island, Japan	Western Pacific	Kyushu Island, Japan		
	5	Outside of Siberia	Mongolia	Gobi Desert	Beijing and Tianjin[d]	
Summer	1	Mongolia	Inner Mongolia[b]	Liaoning[c]	Eastern side of South Korea	Significant fraction of air masses (55%) are originated or passed over polluted zone of China. The remaining air masses are oceanic in origin. Although air masses concerned with mean trajectory 4 are oceanic in origin, they passed over the polluted zone of China.
	2	Jiangsu[c]	Yellow Sea			
	3	Western Pacific	Kyushu Island, Japan			
	4	South China Sea	Guandong[c]	Fujian[c]	Zhejiang[c]	
	5	Pacific Ocean	Ryukyu Islands, Japan	East China Sea		
Autumn	1	Mongolia	Inner Mongolia[b]	Jilin	Southern side of South Korea	Only 40% of air masses are originated from China (mean trajectory 1) while the remaining 38% and 22% are from Siberia (mean trajectory 2 and 4) and Ocean (mean trajectory 3 and 5). Mean trajectories concerned with 1, 2 and 4 pass over the polluted area of China.
	2	Western Siberia	North eastern Mongolia	Liaoning[c]	Eastern side of South Korea	
	3	Pacific Ocean	Ryukyu Islands, Japan			
	4	Western Siberia	Mongolia	Inner Mongolia[b]	Liaoning[c]	
	5	Pacific Ocean	Ryukyu Islands, Japan			
Winter	1	Western Siberia	North eastern Mongolia	Inner Mongolia[b]	Liaoning[c]	Majority of air masses (80%) are originated from Siberia (mean trajectory 1, 2, 4 and 5) but pass through polluted areas of China. 20% of air masses (mean trajectory 3) are originated in Mongolia and passed over the polluted area of China.
	2	Western Siberia	Inner Mongolia[b]	Beijing and Tianjin[d]	Shangdong[c]	
	3	Mongolia	Inner Mongolia[b]	Hebei[c]	Shangdong[c]	
	4	Eastern Siberia	Inner Mongolia[b]	Liaoning[c]		
	5	Outside of Siberia	Mongolia	Inner Mongolia[c]	Liaoning[a]	

[a]The name of places inscribed with superscripts a, b, and c are the provinces of China, except Beijing and Tianjin. These two cities fall within Hebei province.
[b]Less populated and industrialized.
[c]Coastal, heavily populated, and industrialized.
[d]Heavily populated and industrialized.

37), 73 days in summer (n = 13), 54 days in autumn (n = 10), and 91 days in winter (n = 24), where, "n" in parenthesis indicates the number of samples. Therefore, the total number of trajectories calculated in spring, summer, autumn, and winter are 468, 292, 216, and 364, respectively.

[24] All the trajectories in each season were separately subjected to cluster analysis using the cluster algorithm of HYSPLIT model. Given a set of trajectories beginning at one location, the cluster analysis will objectively result in subset of trajectories, called clusters that are each different from the other subsets. Figure 4 shows the results of cluster analyses for four seasons. Each trajectory is the mean of a subset of trajectories. The origins and trajectory pathways of mean clusters in different seasons have been summarized in Table 2. On the basis of the mean trajectories, we found that air masses significantly originated from northeastern China, eastern China, or Korean Peninsula. A few percents of air masses in all seasons, except in winter, originate from or pass over Japan, or southern China (Figure 4). The contributions of either convective or advective boundary layer (<2 km) air masses are 16% in spring (mean trajectory 4, Figure 4a), 74% in summer (mean trajectory 1, 3, 4, and 5; Figure 3b), 23% in autumn (mean trajectory 3 and 4; Figure 4c) and 37% in winter (mean trajectory 1; Figure 4d). All the remaining air masses are descended to the boundary layer at sampling site by convection or advection from the free troposphere (>2 km) (Figure 4). Cluster analysis also suggests that a long-range atmospheric transport not only from East Asia but also from Siberia should be important in determining the chemical and isotopic composition of aerosols at Gosan site.

3. Results and Discussion

3.1. Seasonality of Total Nitrogen (TN), NH_4^+, and NO_3^-

[25] Table 3 summarizes the analytical results of TN, NH_4^+*-N, and NO_3^-*-N measured by EA and NH_4^+ and NO_3^- along with other chemical species. Figure 5 shows the seasonal variations of TN, NH_4^+*-N, NO_3^-*-N, NH_4^+-N, and NO_3^--N in aerosol samples. Generally, all of these chemical species show similar seasonal trend with spring and winter maxima, and summer and autumn minima. The highest TN

Table 3. Summary of Analytical Results of Atmospheric Aerosols Collected at Gosan Site for Four Seasons[a]

Components	Spring (n = 37)		Summer (n = 13)		Autumn (n = 10)		Winter (n = 24)		All Seasons	
	Range	Average[b]	Range	Average[b]	Range	Average[b]	Range	Average[b]	Range	Average[b]
Bulk Analyses										
Aerosol mass (μg m^{-3})	42–268	99 ± 46	33–168	84 ± 43	27–101	61 ± 27	34–155	84 ± 29	27–268	82 ± 36
TN (μg m^{-3})	0.9–6.9	3.1 ± 1.6	0.5–4.4	2.4 ± 1.3	0.2–3.7	1.6 ± 1	0.9–9	2.8 ± 1.8	0.2–9	2.5 ± 1.4
NH_4^+*-N (μg m^{-3})	0.5–5.2	2.2 ± 1.2	0.2–3.7	1.8 ± 1.1	0.1–2.4	0.9 ± 0.8	0.5–5.6	1.8 ± 1.2	0.1–5.6	1.7 ± 1.1
NO_3^-*-N (μg m^{-3})	0.2–2.3	0.9 ± 0.5	0.2–1.7	0.6 ± 0.4	0.1–1.3	0.7 ± 0.4	0.3–3.5	1 ± 0.7	0.1–3.5	0.8 ± 0.5
TN/aerosol mass (%)	0.7–7.3	3.5 ± 1.8	0.9–6	2.9 ± 1.5	2.3–4.5	3.1 ± 0.7	1.4–6.8	3.2 ± 1.4	0.7–7.3	3.2 ± 1.4
Isotope Analyses (‰)[c]										
δ^{15}N (TN)	+8.3 to +23.7	+14.7 ± 3.4	+12 to +26.9	+16.9 ± 4.5	+9.9 to +18.1	+15.8 ± 2.4	+6.8 to +19.4	+12.9 ± 3.4	+6.8 to +26.9	+15.1 ± 3.4
δ^{15}N (NH_4^+*)	+9.9 to +32.2	+17.2 ± 4.6	+13.7 to +29.8	+20.2 ± 5.2	+9.5 to +25.3	+20.7 ± 4.5	+4 to +19.9	+11.3 ± 5.1	+4 to +32.2	+17.4 ± 4.9
δ^{15}N (NO_3^-*)	+1.8 to +15.7	+9.5 ± 3.7	+1.7 to +13.6	+8.3 ± 3.7	+5.6 to +18.1	+12.2 ± 4.1	+9.7 to +21.6	+15.9 ± 3.2	+1.7 to +21.6	+11.5 ± 3.7
Ion analyses ($\mu g\ m^{-3}$)										
Na^+	0.5–12	3.1 ± 2.5	0.7–5.1	2.4 ± 1.1	0.2–5.4	3.4 ± 1.6	1.1–10	5.2 ± 2.1	0.2–12	3.5 ± 1.8
NH_4^+	0.4–6.1	2.4 ± 1.4	0.3–4	1.2 ± 1.2	0.1–2.7	1.2 ± 0.9	0.6–4.7	1.9 ± 1.1	0.1–6.1	1.7 ± 1.2
K^+	0.1–1.1	0.5 ± 0.3	0.2–0.7	0.4 ± 0.2	0.03–0.6	0.3 ± 0.2	0.2–2	0.7 ± 0.4	0.03–2	0.5 ± 0.3
Mg^{2+}	0.08–1.2	0.5 ± 0.3	0.2–0.6	0.3 ± 0.1	0.03–0.7	0.4 ± 0.2	0.3–1.8	0.7 ± 0.3	0.03–1.8	0.5 ± 0.2
Ca^{2+}	0.06–4.7	1.1 ± 1.1	0.1–0.5	0.3 ± 0.1	0.06–0.7	0.3 ± 0.2	0.2–2.9	1.1 ± 0.8	0.06–4.7	0.7 ± 0.6
NO_3^-	1.2–11.7	5.3 ± 2.9	0.9–9.9	3.1 ± 2.3	0.7–8.8	3.6 ± 2.3	1.2–19.5	5.6 ± 4.1	0.7–19.5	4.4 ± 2.9
SO_4^{2-}	2.2–23.1	10.5 ± 5.3	4.8–14.1	9.5 ± 3.5	0.4–11.9	6.5 ± 3.5	4.5–20.7	10.7 ± 3.8	0.4–23.1	9.3 ± 4
Contribution to TN (%)										
NH_4^+	29.7–80.3	59.7 ± 14	34.9–82	59.6 ± 13.3	25.8–75.6	49.7 ± 15.5	41.7–72.8	56.3 ± 8.9	25.8–82	56.3 ± 13
NO_3^-	16.4–74.1	39.6 ± 15.4	17.7–63.6	31.6 ± 15.2	37.5–83.8	54 ± 15.4	26.5–61.4	44 ± 9.8	16.4–83.8	42.3 ± 14

[a] NH_4^+*-N, NO_3^-*-N and their δ^{15}N were not explicitly measured but were measured using a chemical method. See the text for details. The seasons are defined as March–May (spring), June–August (summer), September–November (autumn), and December–February (winter).

[b] Numerical average and standard deviation (±1 SD).

[c] One sample in each spring, summer and winter is excluded in calculating the average δ^{15}N for TN and NO_3^-*. See the text for details.

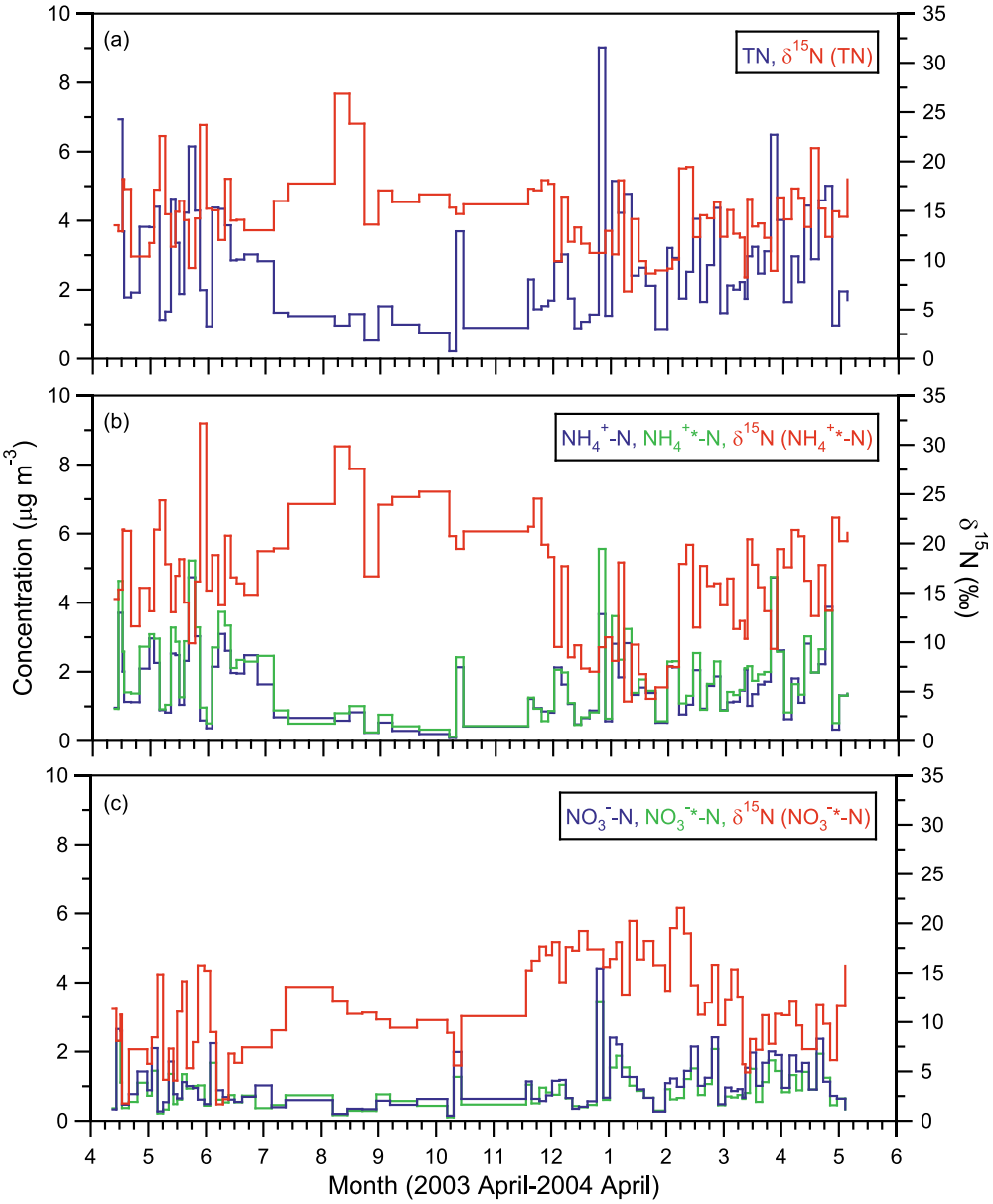

Figure 5. Seasonal variation in the concentrations of (a) total nitrogen (TN) and its $\delta^{15}N$; (b) NH_4^+-N and NH_4^+*-N and its $\delta^{15}N$; and (c) NO_3^--N and NO_3^-*-N and its $\delta^{15}N$ in marine aerosols at Gosan collected from April 2003 to April 2004. NH_4^+*-N, NO_3^-*-N and their $\delta^{15}N$ were not explicitly measured but were measured using a chemical method. See the text for details.

concentration (9 $\mu g\ m^{-3}$) was found in winter whereas the lowest concentration (0.21 $\mu g\ m^{-3}$) was found in autumn. The average concentrations of TN and NH_4^+*-N were found to be the highest in spring (3.1 and 2.2 $\mu g\ m^{-3}$, respectively) followed by winter (2.8 and 1.8 $\mu g\ m^{-3}$), summer (2.4 and 1.8 $\mu g\ m^{-3}$), and autumn (1.6 and 0.9 $\mu g\ m^{-3}$) (Table 3). In contrast, the average concentration of NO_3^-*-N showed the highest in winter (1 $\mu g\ m^{-3}$) followed by spring (0.9 $\mu g\ m^{-3}$), autumn (0.7 $\mu g\ m^{-3}$), and summer (0.6 $\mu g\ m^{-3}$).

[26] Seasonal variations in the concentrations of NH_4^+-N and NO_3^--N measured by ion chromatography are shown in Figure 5. Their variations are quite consistent with NH_4^+*-N and NO_3^-*-N measured by EA. The highest value (6.1 $\mu g\ m^{-3}$) of NH_4^+ was found in a spring sample. In contrast, NO_3^- showed the highest value (19.5 $\mu g\ m^{-3}$) in a winter sample (Table 3). The highest mean concentration of NH_4^+ was found in spring (2.4 $\mu g\ m^{-3}$) followed by winter (1.9 $\mu g\ m^{-3}$) whereas the lowest mean concentrations were observed in summer (1.2 $\mu g\ m^{-3}$) and autumn (1.2 $\mu g\ m^{-3}$). In contrast, the highest mean concentration of NO_3^- (5.6 $\mu g\ m^{-3}$) was found in winter followed by spring (5.3 $\mu g\ m^{-3}$) and autumn (3.6 $\mu g\ m^{-3}$) (Table 3). The lowest mean concentration (3.1 $\mu g\ m^{-3}$) was recorded in summer.

[27] According to one-way ANOVA (analysis of variance), the statistical significances for the measured nitrogenous aerosol components (TN, NH_4^+*-N, NO_3^-*-N, NH_4^+ and NO_3^-) between the seasons range from 0.03 to 0.08. However, these results do not tell us which seasons are

responsible for these differences. Therefore, we carried out two post hoc (Tukey and Gabriel) tests. According to these tests, significant ($p < 0.05$) differences were observed in the mean values of TN, NH_4^+*-N, and NH_4^+ between spring and autumn. There are also significant differences in the mean values of NO_3^-*-N and NO_3^- between spring, winter and other seasons.

[28] TN concentrations (0.2–9 $\mu g\ m^{-3}$, av. 2.5 $\mu g\ m^{-3}$) of this study are comparable with those (0.6–16 $\mu g\ m^{-3}$, av. 3.1 $\mu g\ m^{-3}$) reported for aerosol samples collected from April 2001 to March 2002 at Gosan site [*Kawamura et al.*, 2004]. The contributions of TN to aerosol mass range from 0.7% to 7.3% with an annual mean of 3.2% (Table 3). The concentrations of NH_4^+ range from 0.1 to 6.1 $\mu g\ m^{-3}$ (av. 1.7 $\mu g\ m^{-3}$), whereas those of NO_3^- range from 0.7 to 19.5 $\mu g\ m^{-3}$ (av. 4.4 $\mu g\ m^{-3}$) (Table 3). These results are similar to those (NH_4^+: 0.2–13 $\mu g\ m^{-3}$, av. 2.1 $\mu g\ m^{-3}$ and NO_3^-: 0.2–22 $\mu g\ m^{-3}$, av. 5.3 $\mu g\ m^{-3}$) reported in aerosols collected between April 2001 and March 2002 at Gosan [*Kawamura et al.*, 2004]. The concentrations of NH_4^+ and NO_3^- are reported to be 1.4–3.4 $\mu g\ m^{-3}$ and 1.9–4.2 $\mu g\ m^{-3}$, with annual means of 2.3 and 3 $\mu g\ m^{-3}$, respectively, in Gosan aerosols collected during PEM-West B campaign in 1993 (NASA Langley Atmospheric Sciences Data Center, 2010, http://eosweb.larc.nasa.gov). Although NH_4^+ data of this study as well as the study of *Kawamura et al.* [2004] are similar to those of the PEM-West data, the concentrations of NO_3^- increased from 1993 to 2004 by 60%–77%. This increase in the concentration of NO_3^- over a decade can be interpreted by an increased emission of NO_x (main precursors of NO_3^- in aerosol) in East Asia, particularly in China, from which a major fraction of air masses are transported to Gosan site (Figure 4). This result is consistent with an increased column concentration of NO_2 in eastern China (e.g., Shangdong and Jiangsu) observed by satellite [*Richter et al.*, 2005].

[29] Higher concentrations of TN and NH_4^+ in spring than in summer are consistent with the fact that almost all of the air masses in spring are originated from the free troposphere and then transported from the heavily polluted regions in East Asia (Figure 4a and Table 2). The lower concentrations in summer are due to an increased clean air mass transport from the Sea of Philippine, Pacific Ocean, and South China Sea (Figure 4b and Table 2). Lower concentrations in autumn than in summer are associated with the enhanced free tropospheric transport of air masses from long distances (Figure 4c and Table 2). Although major fraction of air masses in winter are descended to the boundary layer and then transported far away from East Asia, they passed over northeastern provinces of China (Figure 4d and Table 2), where emissions from coal and other fossil- and bio-fuel combustion increase significantly in winter (Beijing Statistical Bureau, http://www.bjstats.gov.cn). That is why we have observed the highest mean concentration of NO_3^- in winter although the concentrations of other species showed the lower values in winter than in spring.

3.2. Seasonality of the $\delta^{15}N$ for Total Nitrogen (TN), NH_4^+*, and NO_3^-*

[30] The $\delta^{15}N$ values of TN, NH_4^+*, and NO_3^-* showed a wide variability among the samples (Figure 5). The $\delta^{15}N$ of TN range from +8.3‰ to +23.7‰ (av. +14.7‰) in spring, +12‰ to +26.9‰ (av. +16.9‰) in summer, +9.9‰ to +18.1‰ (av. +15.8‰) in autumn, and +6.8‰ to +19.4‰ (av. +12.9‰) in winter (Table 3). In calculating the average $\delta^{15}N$ of TN, we excluded three samples KOS 178, 197, and 220 in spring, summer, and winter, respectively, as they showed unexpectedly higher values, which have never been reported in literature. A significant statistical difference ($p < 0.05$) was observed in the mean $\delta^{15}N$ values between summer and winter.

[31] The lowest mean $\delta^{15}N$ of TN in winter can be partly interpreted by more contribution of TN from coal burning because the particles produced by the combustion of coal are generally more depleted in ^{15}N ($\delta^{15}N < 0$) in comparison to other sources (gasoline, natural gas and waste incinerators) (Figure 6a, top) [*Widory*, 2007]. The consumption of coal is significantly enhanced in winter in East Asia, especially in China (http://www.bjstats.gov.cn) and air mass transport patterns also suggest that most of the air masses in winter are transported to Gosan site from northeastern China (Figure 4d). But the $\delta^{15}N$ values of TN and NH_4^+* observed are significantly higher in winter than those of primarily emitted aerosol nitrogen from the combustion of coal and other fossil fuels, except for bio-fuels (Figure 6a). This suggests that the combustion-derived nitrogen is diluted by other sources and/or relevant atmospheric chemical processes.

[32] Similar seasonal trends for the $\delta^{15}N$ values of TN were reported for aerosols collected from urban Paris and rural Brazil, pointing out to the similar atmospheric processing of nitrogenous species in the atmosphere. The $\delta^{15}N$ values of TN in aerosols ranged from +7‰ to +18.7‰ at Piracicaba in São Paulo State and from +8.4‰ to +17.4‰ at Santarém in Pará State, Brazil [*Martinelli et al.*, 2002], where the upper limits are lower than our data. In these sites, the $\delta^{15}N$ values are higher than those of vegetation tissues and soil organic matter, which are the potential sources of nitrogen in aerosol particles. The $\delta^{15}N$ values in Paris aerosols also show the lower range than ours: +5.3‰ to +16.1‰ with mean values of 10.8‰ ± 3.4‰ in summer and 10‰ ± 3.4‰ in winter [*Widory*, 2007]. Our Gosan aerosols showed much broader $\delta^{15}N$ values (+6.8‰ to +26.9‰) than Brazil and Paris aerosols, possibly due to more contributions of anthropogenic activities and atmospheric processing of nitrogenous species during a long-range transport of pollutants from East Asia to Gosan site.

[33] The $\delta^{15}N$ values of NH_4^+* are +9.9‰ to +32.2‰ (av. +17.2‰) in spring, +13.7‰ to +29.8‰ (av. +20.2‰) in summer, +9.5‰ to +25.3‰ (av. +20.7‰) in autumn, and +4‰ to +19.9‰ (av. +11.3‰) in winter (Table 3). There is a significant difference ($p < 0.05$) in the mean $\delta^{15}N$ values of NH_4^+* between winter and other seasons. As seen in Figures 6a and 6b, the mean $\delta^{15}N$ values of TN and NH_4^+* are higher in summer and autumn than in two other seasons. Higher $\delta^{15}N$ in summer and autumn can partly be explained by an enhanced contribution of biomass burning aerosols, which are enriched with ^{15}N (Figure 6a). Actually, summer and autumn are the harvest seasons in China and significant fraction of agricultural straws are burnt [*Wang et al.*, 2009]. Figures 4b and 4c also suggest that 55% (clusters 1 and 2) and 78% (clusters 1, 2 and 4) of total air masses are transported over China in summer and autumn, respectively.

[34] The $\delta^{15}N$ of NO_3^-* ranged from +1.8‰ to +15.7‰ (av. +9.5‰) in spring, +1.7‰ to +13.6‰ (av. +8.3‰) in

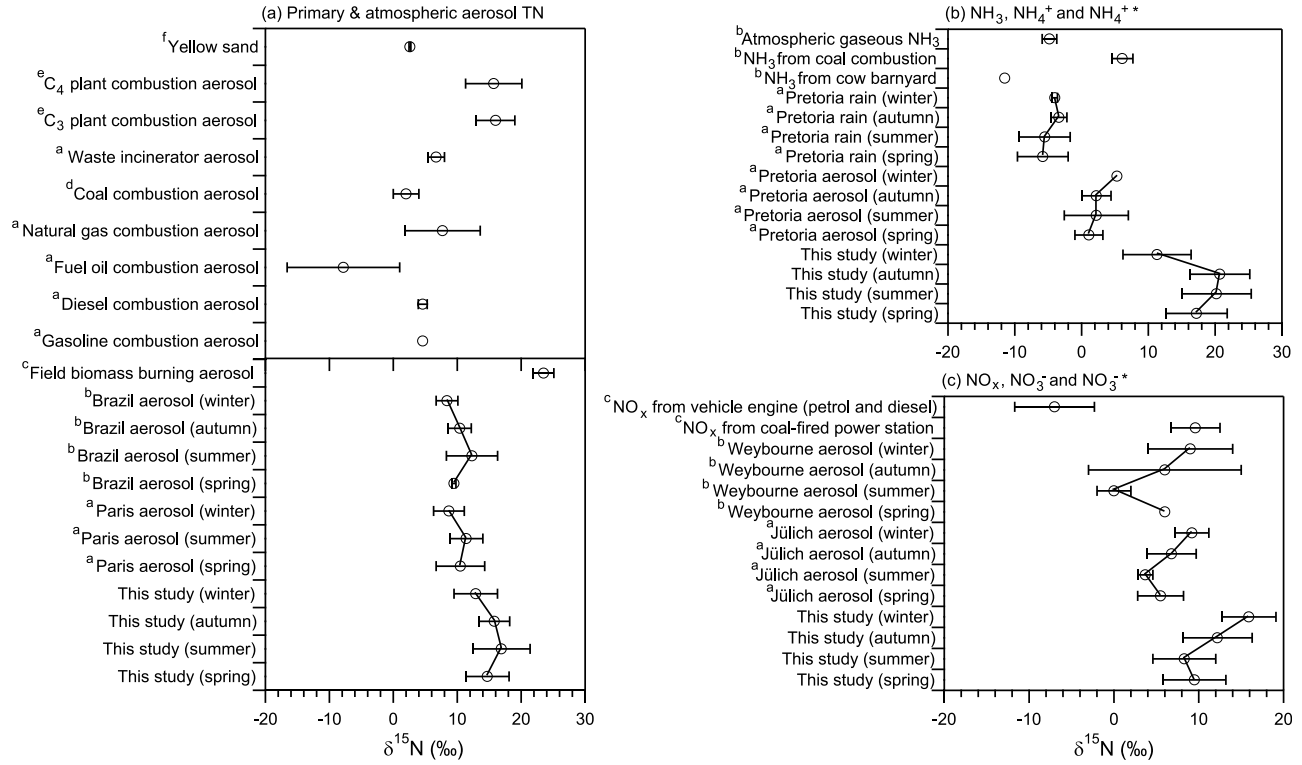

Figure 6. Comparison of seasonal variation of the δ^{15}N of (a) total nitrogen (TN), (b) NH_4^+*, and (c) NO_3^-* of this study with other study results. These figures also show the δ^{15}N signals of primary aerosol nitrogen and gaseous precursors of secondary aerosol nitrogen emitted from major sources. Data marked with superscripts a, b, c, d, e, and f in Figure 7a are cited from *Widory* [2007], *Martinelli et al.* [2002], *Kundu et al.* [2010], *Freyer* [1991], *Turekian et al.* [1998], and *Kawamura et al.* [2004], respectively, whereas data marked with superscripts a and b in Figure 7b are cited from *Heaton* [1987] and *Freyer* [1978b], respectively, and data marked with superscripts a, b and c in Figure 7c are cited from *Freyer* [1991], *Yeatman et al.* [2001b], and *Heaton* [1990], respectively.

summer, +5.6‰ to +18.1‰ (av. +12.2‰) in autumn, and +9.7‰ to +21.6‰ in winter (av. +15.9‰) (Table 3). There exists a significant difference ($p < 0.05$) in the mean δ^{15}N values between winter and the other seasons. Being opposite to the δ^{15}N of NH_4^+*, NO_3^-* showed the lowest mean δ^{15}N values in spring and summer (Figure 6c). These results suggest dominant contributions of NO_x from gasoline and diesel combustion in spring and summer and from coal combustion in winter. The δ^{15}N of NO_x from gasoline and diesel combustion is lower than that from coal combustion (Figure 6c). The seasonal trend of δ^{15}N at Gosan site is similar with the previously reported studies as shown in Figure 6c. For example, the δ^{15}N values of NO_3^- that were reported for coastal aerosol samples from Weybourne (UK) [*Yeatman et al.*, 2001b] and moderately polluted aerosol samples from Jülich (Germany) [*Freyer*, 1991] showed lower mean values in summer than in winter. *Freyer* [1991] explained the seasonal trend in Jülich aerosol considering equilibrium isotope exchange reactions between oxinitrogen species including NO and NO_2, and NO_2 and N_2O_5 in the atmosphere. Their explanation was strongly supported by the higher δ^{15}N of NO_3^- (range: −2‰ to +18‰) than that of NO_2 (range: −15‰ to −5‰).

[35] *Freyer et al.* [1993] observed higher δ^{15}N of NO_2 in winter than in summer in the presence of high concentrations of NO_x (~10–45 ppbv) and moderate concentrations of O_3 (~4 to 40 ppbv) in the atmosphere. This trend was explained by the fact that in this condition in winter, an enhanced equilibrium isotopic exchange occurs between NO_2 and N_2O_5 due to longer nights and reduced photochemical activity. Therefore, the dissociation of N_2O_5 to NO and NO_2 in the daytime produces NO_2 with higher δ^{15}N in winter.

[36] In our study site at Gosan, NO_3^- is transported from China, Korea and Japan (Figure 9), where NO_x levels can exceed ozone levels. Hence, equilibrium isotope exchange could occur between reactive nitrogen species in the atmosphere, which drives the seasonal cycle of δ^{15}N of NO_2 and subsequently δ^{15}N of NO_3^- in Gosan aerosols. Moreover, NO_x concentration generally maximizes and ozone concentration minimizes in winter in East Asian locations [*Han et al.*, 2009; *Li et al.*, 2007] from China, Korea and Japan. This condition favors higher δ^{15}N of NO_2 and NO_3^-. *Freyer et al.* [1993] also observed the higher δ^{15}N of NO_2 when NO_x concentrations exceeded those of O_3.

3.3. Aerosol Chemistry and Its Relation to the δ^{15}N of Nitrogenous Species in Aerosols

[37] On the basis of the Ca^{2+}/Na^+ ratios, we divide our 84 samples into three categories: (1) Na^+ enriched samples, (2)

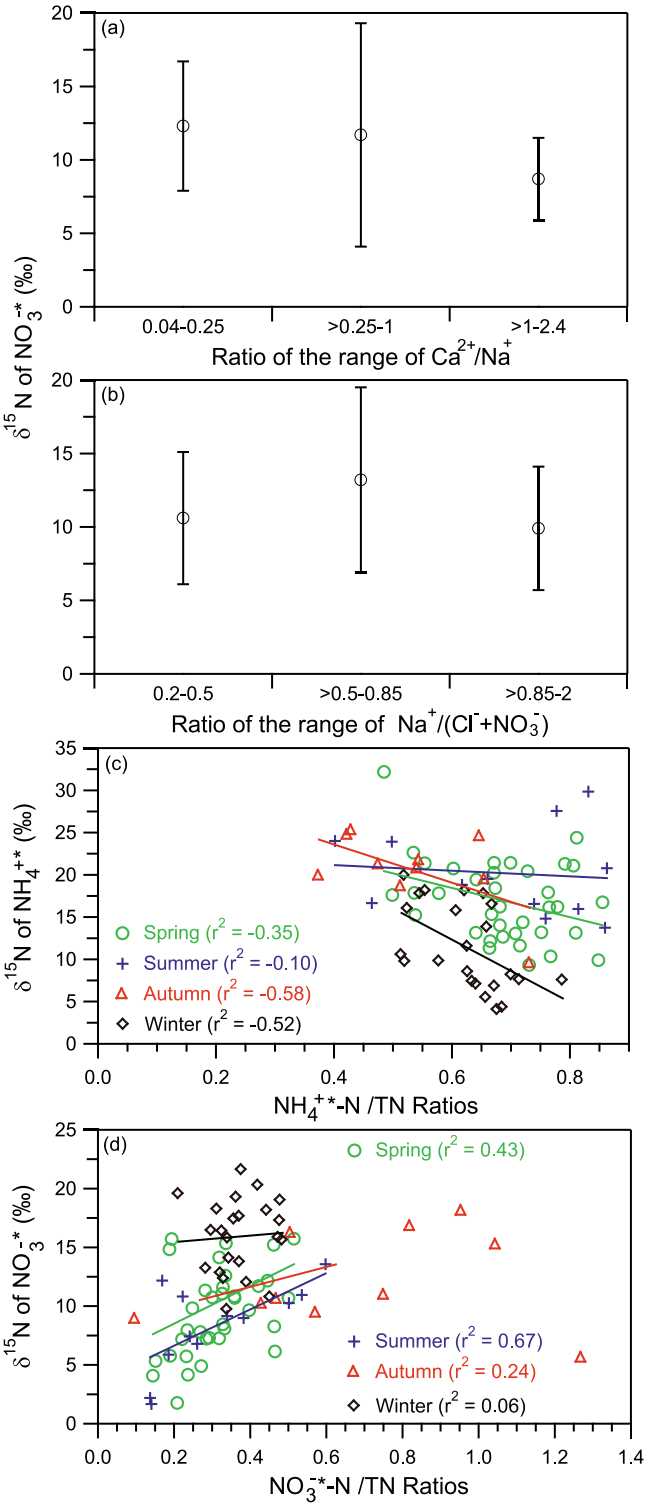

Figure 7. Relation between (a) the δ^{15}N of NO_3^-* and Ca^{2+}/Na^+ ratios, (b) the δ^{15}N of NO_3^-* and $Na^+/(Cl^- + NO_3^-)$ ratios, (c) the δ^{15}N of NH_4^+* and NH_4^+*-N/TN ratios, and (d) the δ^{15}N of NO_3^-* and NO_3^-*-N/TN ratios.

moderately Na^+ enriched samples, and (3) Ca^{2+} enriched samples. NO_3^- predominantly exists in the coarse mode due to the reactions of HNO_3 with sea salt and dust particles. We observed that the mean δ^{15}N of NO_3^-* is higher by 3.6‰ in Na^+ enriched samples than in Ca^{2+} enriched samples, suggesting that ^{15}N-depleted HNO_3 is preferentially taken by Ca^{2+} that may originally exist as $CaCO_3$ and hence NO_3^- produced from this reaction becomes depleted in ^{15}N (Figure 7a). It could also be related with a fact that nitrate, with a different loading of Ca^{2+} and Na^+ in aerosols, is produced from different sources. Nitrogen isotopic discrimination, during NO_3^- formation in the aerosol phase via the reactions between dust/sea-salt particles and HNO_3, has not been reported previously. There is evidence that the δ^{15}N (NO_3^-) (+4.2‰ to +8‰) in the fine aerosols (<3.5 μm) is higher than that (0.6‰–5.5‰) in the coarse aerosols (>3.5 μm) [*Freyer*, 1991]. However, *Morin et al.* [2009] did not observe any significant difference between the δ^{15}N (NO_3^-) from different size classes of aerosols. Therefore, further studies are required to better understand the nitrogen isotopic fractionation during NO_3^- production in the aerosol phase.

[38] $Na^+/(Cl^- + NO_3^-)$ ratio in the aerosols produced from sea spray is 0.85 [*Wall et al.*, 1988; *Zhuang et al.*, 1999]. Any deviation from this ratio is an indication of additional sources and/or atmospheric reactions of Na^+, NO_3^-, and Cl^-. Some coarse Na^+ may originate from soil or combustion sources, and some coarse Cl^- or NO_3^- may evaporate, resulting in ratios >0.85. On the other hand, Na^+ should not evaporate under ambient atmospheric conditions. Thus, the lower ratios observed in our samples are possibly due to the reaction of HNO_3 with dust particles containing Ca^{2+}. The mean δ^{15}N of NO_3^-* for samples with the lowest $Na^+/(Cl^- + NO_3^-)$ ratios (0.2–0.5) is lower by 2.6‰ than that for samples with higher $Na^+/(Cl^- + NO_3^-)$ ratios (0.5–0.85) (Figure 7b). This is consistent with the relation between δ^{15}N of NO_3^-* and higher Ca^{2+}/Na^+ ratios (Figure 7a). $Na^+/(Cl^- + NO_3^-)$ ratios in a number of samples are higher than 0.85, which can be caused by the removal of Cl^- as HCl due to the reactions between H_2SO_4 and NaCl assuming that Na^+ does not have other sources. The average δ^{15}N of NO_3^-* for this sample group is 9.9‰, which is equivalent to the sample group with the lowest $Na^+/(Cl^- + NO_3^-)$ ratios (Figure 7b).

[39] The δ^{15}N values of NH_4^+* were found to decrease with an increase in NH_4^+*-N/TN concentration ratios in aerosols (Figure 7c). In contrast, the δ^{15}N values of NO_3^-* increased with an increase in NO_3^-*-N/TN concentration ratios (Figure 7d). A test of Pearson's correlation ($\alpha = 0.05$) shows that the correlations between NH_4^+*-N/TN and the δ^{15}N are significant in spring ($r^2 = 0.35$, $n = 37$), autumn ($r^2 = 0.58$, $n = 10$), and winter ($r^2 = 0.52$, $n = 24$), except in summer ($r^2 = 0.10$, $n = 13$). Similar statistical test for the correlations between NO_3^-*-N/TN and the δ^{15}N are significant in spring ($r^2 = 0.43$) and summer ($r^2 = 0.67$), but not in autumn ($r^2 = 0.24$) and winter ($r^2 = 0.06$). The trends observed in Figures 7c and 7d may suggest that there exists a difference in the isotopic shift between NH_4^+ and NO_3^- formations. These results may also suggest that the isotopic shift during the formation of secondary aerosol nitrogen depends upon the seasons. Although an inversed relation was observed between TN and its δ^{15}N in urban Paris aerosols in winter, there was a positive relation in summer [*Widory*, 2007]. These trends were explained by season specific secondary aerosol nitrogen formation.

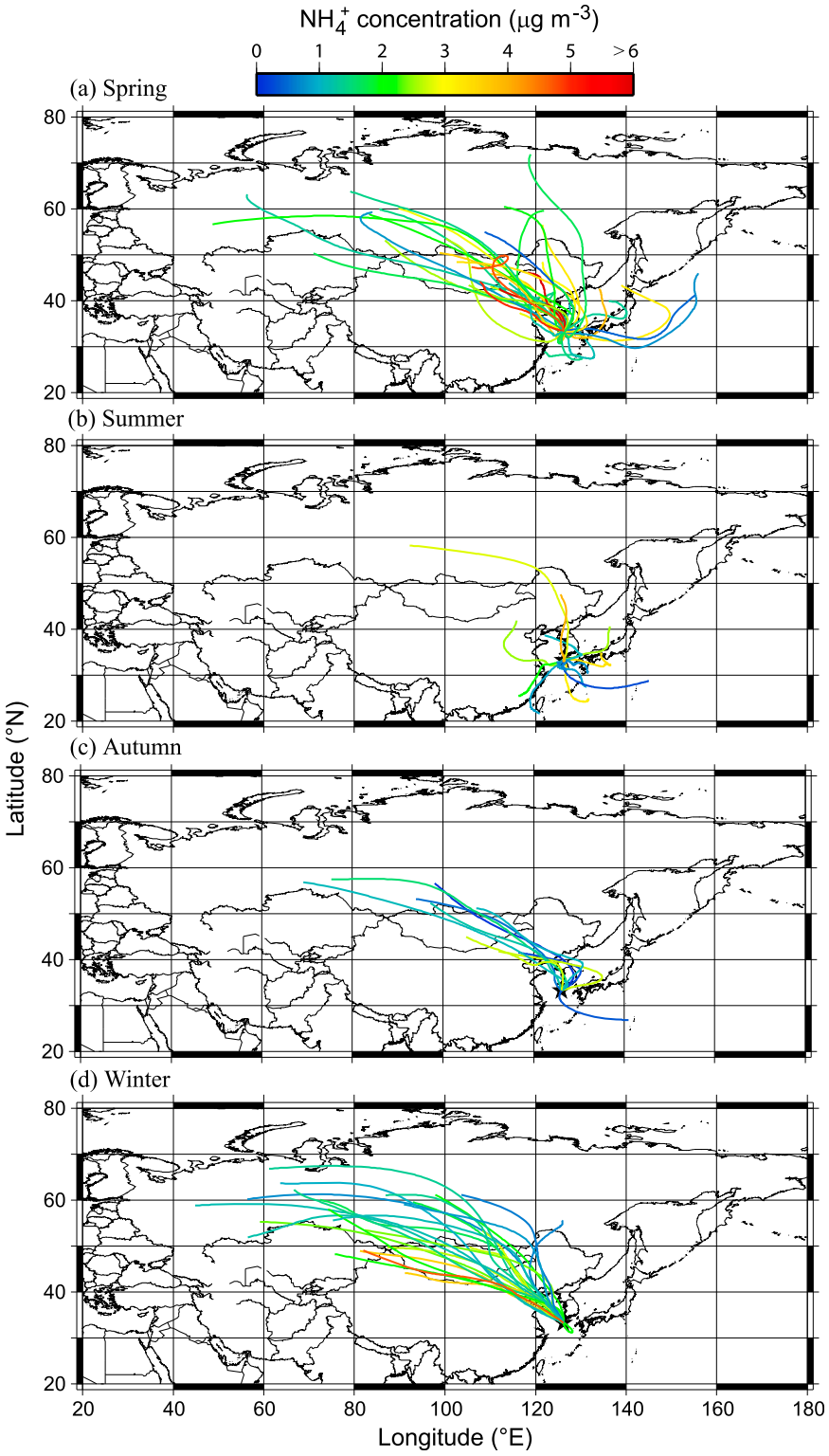

Figure 8. Variability of the concentrations of ammonium (NH_4^+) among trajectories in (a) spring, (b) summer, (c) autumn, and (d) winter. Each sample was collected for a few days. Trajectories were calculated 4 times a day. Therefore, each trajectory is the mean of a number of trajectories. The mean trajectories were colored according to the observed NH_4^+ concentrations at the sampling site. The concentration of a sample in spring goes beyond the upper range of color scale.

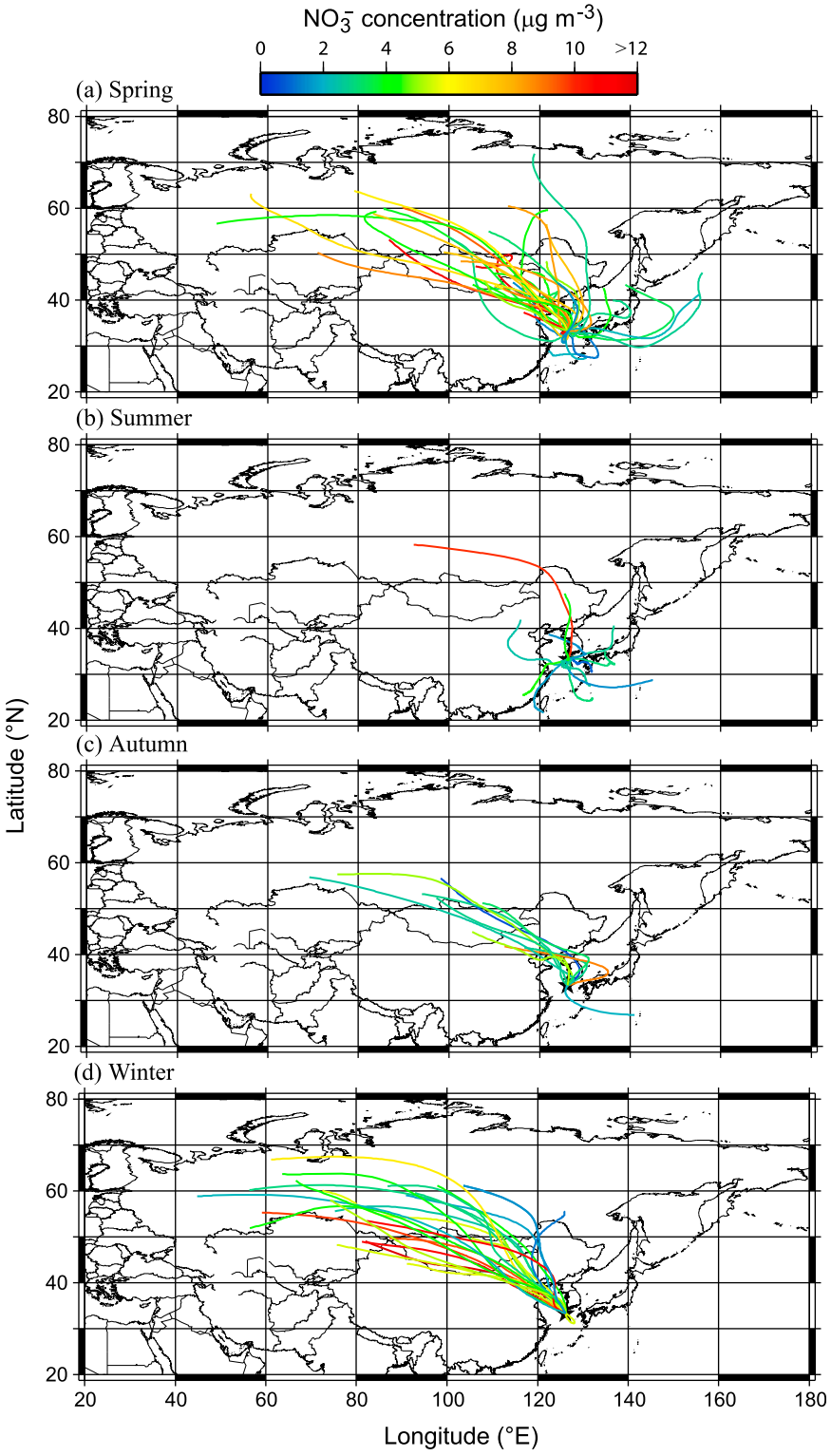

Figure 9. Variability of the concentrations of nitrate (NO_3^-) among trajectories in (a) spring, (b) summer, (c) autumn, and (d) winter. The mean trajectories were colored according to the observed NO_3^- concentrations at the sampling site. The concentration of a sample in winter goes beyond the upper range of color scale.

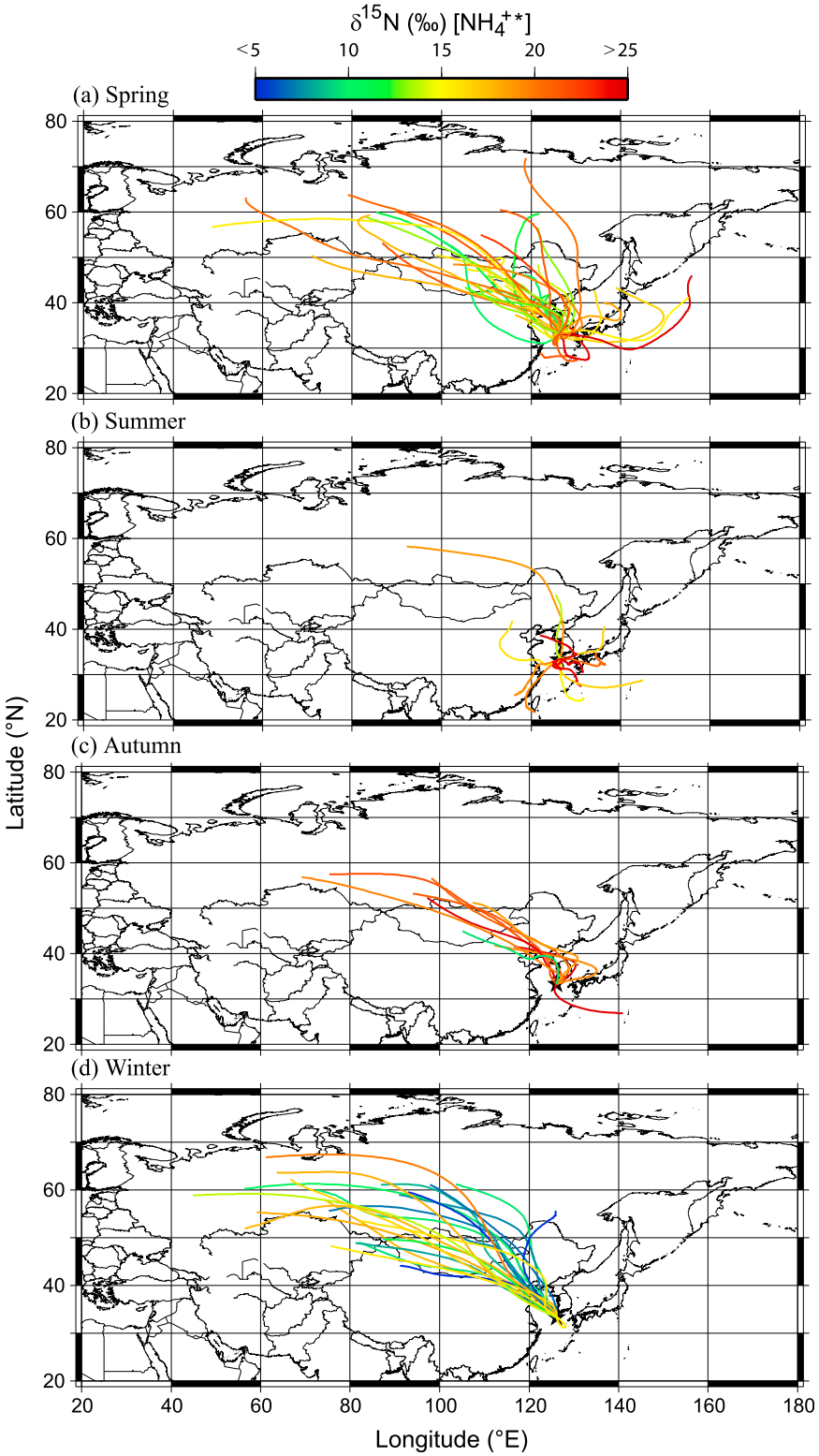

Figure 10. Variability of the $\delta^{15}N$ of NH_4^+* among mean trajectories for (a) spring, (b) summer, (c) autumn, and (d) winter. The $\delta^{15}N$ values of one sample in spring, two samples in summer, and one sample in autumn go beyond the upper range of color scale, whereas the $\delta^{15}N$ values of two samples in autumn go beyond the lower range of color scale.

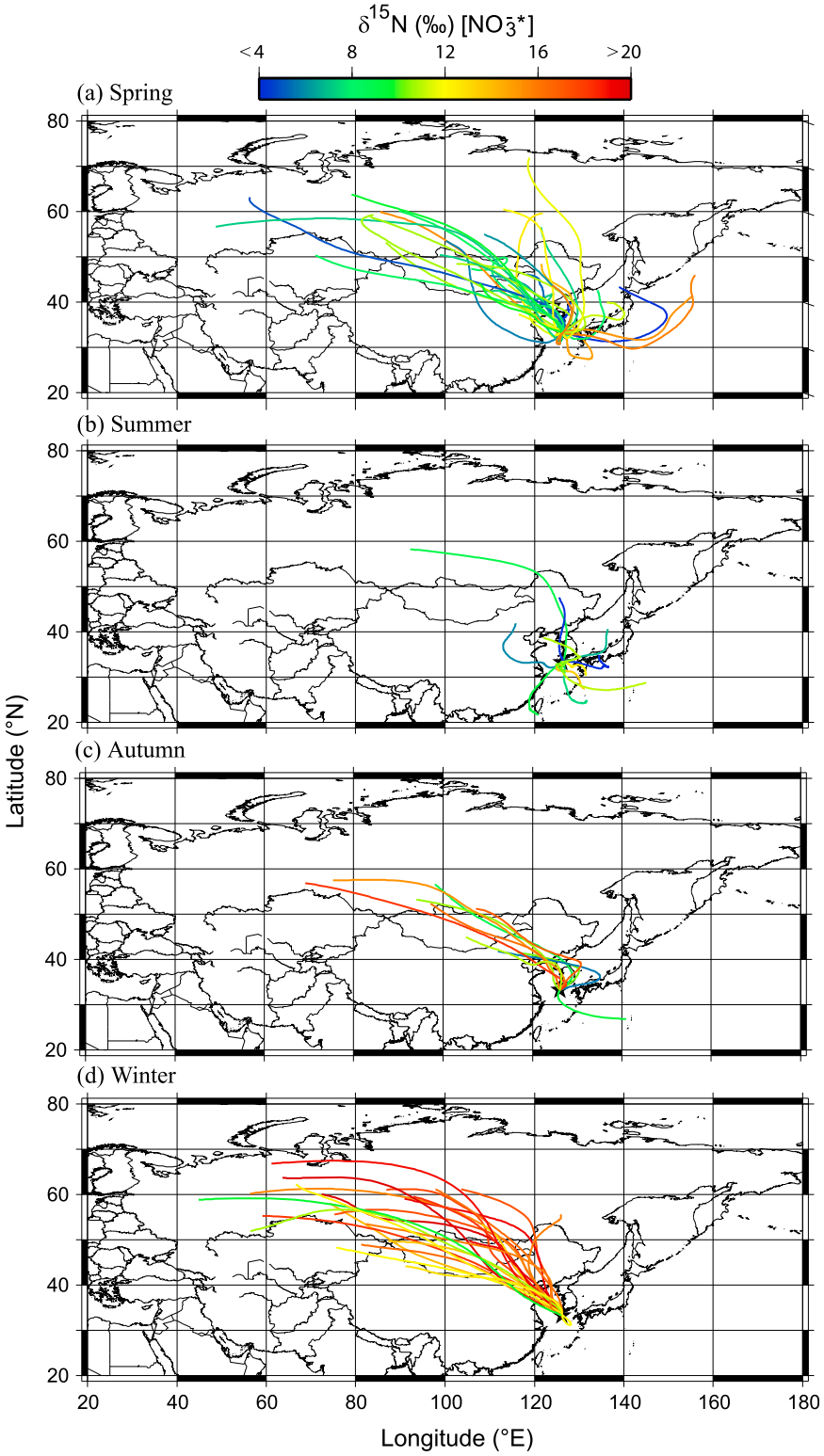

Figure 11. Variability of the $\delta^{15}N$ of NO_3^-* among mean trajectories for (a) spring, (b) summer, (c) autumn, and (d) winter. The $\delta^{15}N$ values of one sample in spring and two samples in summer go beyond the lower range of color scale.

3.4. Unusual Values of the $\delta^{15}N$ of TN and NO_3^-

[40] The $\delta^{15}N$ values of TN for samples KOS 178 in spring, KOS 197 in summer and KOS 220 in winter are +48.9‰, +48.4‰, and +183.6‰, respectively. Although such higher values have not been reported so far, we have confirmed that these values are real based on repeated

analyses (4 times). Interestingly, such high $\delta^{15}N$ values were not observed for NH_4^+* in these samples, suggesting that removed NO_3^- is heavily enriched with ^{15}N. We calculated the $\delta^{15}N$ of NO_3^-* in these samples using isotopic mass balance equation. Unexpectedly high values (KOS 178: +132‰, KOS 197: +244‰ and KOS 220: +464‰) were derived for these samples. Probably, "flash" (really fast) reaction such as denitrification of NO_3^- in atmospheric aerosols, to some extent, could explain such type of higher values of NO_3^-.

[41] Nitrate in groundwater of the western Kalahari of southern Africa is converted to N_2 by bacterial denitrification [*Heaton*, 1985]. The isotopic separation/enrichment factor ($\varepsilon_{product\text{-}reactant}$) for denitrification was found to be −35‰ [*Vogel et al.*, 1981]. *Cline and Kaplan* [1975] reported similar values of −40‰ to −30‰ for oceanic denitrification. Laboratory experiments have produced values from −33‰ to −10‰ depending on the experimental conditions influencing bacterial metabolism [*Mariotti et al.*, 1982]. Because of the denitrification, remaining NO_3^- in aerosols becomes progressively enriched in ^{15}N. But, this requires anaerobic condition. Therefore, we need to assume that aerosols in those samples could be coated with hydrophobic materials that create a barrier of microlayer to prevent the penetration of oxygen from the air into aerosols. Further studies are required to explain these unexpectedly high $\delta^{15}N$ values in the future.

3.5. Variability of Chemical and Isotopic Composition Among Trajectory Types

[42] To characterize the observed NH_4^+ and NO_3^- in the different air masses encountered during the collection of samples, the mean air mass back trajectory for each sample was calculated. The most of the air mass trajectories are generally tagged with higher concentrations of NH_4^+ in spring, summer and winter (Figure 8). For example, only 19%, 46%, and 33% of samples in spring, summer and winter, respectively, showed lower concentrations of NH_4^+ than the observed mean concentration of NH_4^+ in autumn. Most of the air mass trajectories in autumn, except for 3, originated from Siberia with a transport pathway over northeast China. This result suggests that NH_4^+ transport from northeast China to Gosan is significantly reduced in autumn.

[43] Although the variability in NO_3^- concentrations among the trajectories is similar to NH_4^+ in spring and winter, there is a difference in summer and autumn (Figure 9). Majority of the air masses are characterized by lower concentrations of NO_3^- in summer than in autumn. Only 27% samples in spring and 33% samples in winter showed the concentrations lower than the observed mean concentration in summer. Although air mass transport patterns in winter and autumn are very similar, only a few samples in winter showed the concentrations of NO_3^- to be lower than the mean concentration of NO_3^- in autumn. Thus, the present study indicates that northeast China as well as Siberia is an important source region for NO_3^- in winter aerosols.

[44] Higher $\delta^{15}N$ values of NH_4^+* in warm season (March–August) are characterized by the trajectories arriving at Gosan site from the east, southeast, south, southwest, and by the stagnant air masses that remain in the vicinity of Jeju Island (hereafter referred to as S/SE/SW transport) (Figure 10). In contrast, lower $\delta^{15}N$ in cold season (September–February) is characterized by the rapid transport of air parcels from northeastern China and Siberia to the west and northwest of Gosan site due to strong westerlies (hereafter referred to as W/NW transport).

[45] The mean $\delta^{15}N$ of NH_4^+* during S/SE/SW transport in warm season (March–August) is higher by 7.4‰ than that during W/NW transport in the later half of cold season (winter: November–February) (Table 3). We expected to find lower $\delta^{15}N$ values of NH_4^+* for S/SE/SW transport because of the preferential emission of $^{14}NH_3$ over $^{15}NH_3$ in warm season from soil, fertilizer, and animal excreta [*Russell et al.*, 1998], as depicted in Figure 6b for lower $\delta^{15}N$ values of NH_4^+ in aerosol and rain samples of Pretoria, South Africa. However, higher $\delta^{15}N$ values for the samples of S/SE/SW transport and for the samples of the first half of W/NW (autumn) transport were found in Gosan site (Figures 10a, 10b, and 10c), again suggesting that an increased emissions from biomass burning and some relevant atmospheric chemical processes may determine the nitrogen isotopic ratios of the NH_4^+. The isotopic fractionation under equilibrium conversion of $NH_{3(gas)}$ to $NH_{4(aqueous)}^+$ may likely occur, which was estimated to be in the range of +25‰ to +35‰ [*Mariotti et al.*, 1984; *Heaton*, 1987]. This estimation can be supported by higher $\delta^{15}N$ of NH_4^+ in atmospheric aerosols collected from barnyard [*Yeatman et al.*, 2001b].

[46] The mean $\delta^{15}N$ value of NO_3^-* during S/SE/SW transport in warm season is lower by 5.6‰ than that during W/NW transport in cold season (Table 3 and Figure 11). Higher $\delta^{15}N$ values of NO_3^-* in W/NW transport can be explained by an enhanced contribution of NO_x from coal (NO_x from coal combustion is enriched with ^{15}N, see Figure 6c) and by the difference in NO_x scavenging mechanism between warm and cold seasons. The enhanced contribution of coal NO_x is associated with its increased consumption; e.g., total residential energy consumption in Beijing during cold season is 54% higher than that of warm season in 2006 (http://www.bjstats.gov.cn). The NO_3^- produced via an enhanced reaction between NO_x and OH radicals in warm season is depleted with ^{15}N whereas it is enriched with ^{15}N produced via an enhanced reaction between NO_x and NO_3 radicals in cold season [*Freyer et al.*, 1993].

4. Conclusions

[47] We found that total nitrogen (TN) concentrations in atmospheric aerosols collected from Gosan site, Jeju Island, are high (0.2–9 $\mu g\ m^{-3}$) with an average of 2.5 $\mu g\ m^{-3}$, in which TN is mainly composed of NH_4^+ (annual mean: 56.3%) followed by NO_3^- (42.3%). Significant seasonal variations of the $\delta^{15}N$ of TN, NH_4^+*, and NO_3^-* were found in the Gosan aerosols, which we interpreted by seasonal differences in the sources and chemical processing of nitrogenous species in the atmosphere. It appears that lower $\delta^{15}N$ values of NO_3^-* are caused by less isotopic enrichment ($\varepsilon_{product\text{-}reactant}$) during the reactions between HNO_3 and dust particles. This study also demonstrates that a significant isotopic enrichment of ^{15}N occurs in aerosols during the gas-to-particle conversion ($NH_3 \rightarrow NH_4^+$) and the subsequent gas/aerosol partitioning of nitrogenous species. We propose that the $\delta^{15}N$ of the different species in aerosols is

useful tool to interpret the secondary production of aerosol nitrogen in the atmosphere and to better understand the changes in the sources and source strengths of nitrogenous species in the atmosphere with seasons.

[48] **Acknowledgments.** This study was in part supported by the Japanese Ministry of Education, Science, Sport and Culture (MEXT) through grants-in-aid 14204025 and 17340166 and the Environment Research and Technology Development Fund (B-0903) of the Ministry of Environment, Japan. S.K. acknowledges financial support from the MEXT. The authors are grateful to NOAA Air Resources Laboratory (ARL) for allowing the installation of registered version of Windows-based HYSPLIT model. We are also grateful to NASA Langley Atmospheric Sciences Data Center for supplying the data in a CD-ROM for PEM-West A and PEM-West B campaigns.

References

Allen, A. G., R. M. Harrison, and J. W. Erisman (1989), Field measurements of the dissociation of ammonium nitrate and ammonium chloride, *Atmos. Environ.*, *23*, 1591–1599.

Brimblecombe, P., and S. L. Clegg (1988), The solubility and behaviour of acid gases in the marine aerosol, *J. Atmos. Chem.*, *7*, 1–18.

Carmichael, G. R., Y. Zhang, L.-L. Chen, S. M. Hong, and H. Ueda (1996), Seasonal variation on aerosol composition at Cheju Island, Korea, *Atmos. Environ.*, *30*, 2407–2416.

Carmichael, G. R., M.-S. Hong, H. Ueda, L.-L. Chen, K. Murano, J. K. Park, Y. Lee, C. Kang, and S. Shim (1997), Aerosol composition at Cheju Island, Korea, *J. Geophys. Res.*, *102*, 6047–6061, doi:10.1029/96JD02961.

Chen, L.-L., et al. (1997), Influence of continental outflows on the aerosol composition at Cheju Island, South Korea, *J. Geophys. Res.*, *102*, 28,551–28,574, doi:10.1029/97JD01431.

Clegg, S. L., P. Brimblecombe, and A. S. Wexler (1998), Thermodynamic model of the system H^+-NH_4^+-SO_4^{2-}-NO_3^--H_2O at tropospheric temperatures, *J. Phys. Chem.*, *102*, 2137–2154.

Cline, J. D., and I. R. Kaplan (1975), Isotopic fractionation of dissolved nitrate during denitrification in the eastern tropical North Pacific Ocean, *Mar. Chem.*, *3*, 271–299.

Draxler, R. R., B. Stunder, G. Rolph, and A. Taylor (2006), HYSPLIT4 user's guide, *Nation. Ocean. and Atmos. Adminis. Tech. Memo. ERL ARL-230*. (Available at http://www.arl.noaa.gov/dataweb/models/hysplit4/win95/user_guide.pdf)

Duce, R. A., et al. (2008), Impacts of atmospheric anthropogenic nitrogen on the open ocean, *Science*, *320*, 893–897.

Freyer, H. D. (1978a), Seasonal trends of NH_4^+ and NO_3^- nitrogen isotopic composition in rain collected at Jülich, Germany, *Tellus*, *30*, 83–92.

Freyer, H. D. (1978b), Preliminary $\delta^{15}N$ studies on atmospheric nitrogenous trace gases, *Pure Appl. Geophys.*, *116*, 393–404.

Freyer, H. D. (1991), Seasonal variation of $^{15}N/^{14}N$ ratios in atmospheric nitrate species, *Tellus*, *43B*, 30–44.

Freyer, H. D., D. Kelly, A. Voltz-Thomas, and K. Kobel (1993), On the interaction of isotope exchange process with photochemical reactions in atmospheric oxides of nitrogen, *J. Geophys. Res.*, *98*, 14,791–14,796, doi:10.1029/93JD00874.

Galloway, J. N., and G. E. Likens (1981), Acid precipitation: The importance of nitric acid, *Atmos. Environ.*, *15*, 1081–1085.

Galloway, J. N., W. H. Schlesinger, H. Levy, A. Michaels, and J. L. Schnoor (1995), Nitrogen fixation; anthropogenic enhancement-environmental response, *Global Biogeochem. Cycles*, *9*, 235–252, doi:10.1029/95GB00158.

Gao, Y. (2002), Atmospheric deposition to Barnegat Bay, *Atmos. Environ.*, *36*(38), 5783–5794.

Han, K. M., C. H. Song, H. J. Ahn, R. S. Park, J. H. Woo, C. K. Lee, A. Richter, J. P. Burrows, J. Y. Kim, and J. H. Hong (2009), Investigation of NO_x emissions and NO_x-related chemistry in East Asia using CMAQ-predicted and GOME-derived NO_2 columns, *Atmos. Chem. Phys.*, *9*, 1017–1036.

Harrison, R. M., and C. Pio (1983), Size differentiated composition of inorganic atmospheric aerosols of both marine and polluted continental origin, *Atmos. Environ.*, *17*, 1733–1738.

Harrison, R. M., and A. R. MacKenzie (1990), A numerical simulation of kinetic constraints upon achievement of the ammonium nitrate dissociation equilibrium in the troposphere, *Atmos. Environ.*, *24A*, 91–102.

Hastings, M. G., D. M. Sigman, and F. Lipschultz (2003), Isotopic evidence for source changes of nitrate in rain at Bermuda, *J. Geophys. Res.*, *108*(D24), 4790, doi:10.1029/2003JD003789.

Hayami, H., and G. R. Carmichael (1997), Analysis of aerosol composition at Cheju Island, Korea, using a two-bin gas-aerosol equilibrium model, *Atmos. Environ.*, *31*, 3429–3439.

Hayami, H., and G. R. Carmichael (1998), Factors influencing the seasonal variation in particulate nitrate at Cheju Island, South Korea, *Atmos. Environ.*, *32*, 1427–1434.

Heaton, T. H. E. (1985), Isotopic and chemical aspects of nitrate in the ground water of the springbok Flats, *Water S. Afr.*, *11*, 199–208.

Heaton, T. H. E. (1986), Isotopic studies of nitrogen pollution in the hydrosphere and atmosphere: A review, *Chem. Geol. (Isotope Geoscience Section)*, *59*, 87–102.

Heaton, T. H. E. (1987), $^{15}N/^{14}N$ ratios of nitrate and ammonium in rain at Pretoria, South Africa, *Atmos. Environ.*, *21*, 843–852.

Heaton, T. H. E. (1990), $^{15}N/^{14}N$ ratios of NO_x from vehicle engines and coal fired power stations, *Tellus*, *42B*, 304–307.

Hoell, J. M., D. D. Davis, S. C. Liu, R. Newell, M. Shipham, H. Akimoto, R. J. McNeal, R. J. Bendura, and J. W. Drewry (1996), Pacific Exploratory Mission-West A (PEM-WEST A): September–October 1991, *J. Geophys. Res.*, *101*, 1641–1653, doi:10.1029/95JD00622.

Hoell, J. M., D. D. Davis, S. C. Liu, R. E. Newell, H. Akimoto, R. J. McNeal, and R. J. Bendura (1997), The Pacific Exploratory Mission-West Phase B: February–March, 1994, *J. Geophys. Res.*, *102*, 28,223–28,239, doi:10.1029/97JD02581.

Hoering, T. (1957), The isotopic composition of ammonia and the nitrate ion in rain, *Geochim. Cosmochim. Acta.*, *12*, 97–102.

Huebert, B. J., T. Bates, P. B. Russel, G. Y. Shi, Y. J. Kim, K. Kawamura, G. Carmichael, and T. Nakajima (2003), An overview of ACE-Asia: Strategies for quantifying the relationships between Asian aerosols and their climate impacts, *J. Geophys. Res.*, *108*(D23), 8633, doi:10.1029/2003JD003550.

Jickells, T. D. (1998), Nutrient biogeochemistry of the coastal zone, *Science*, *281*, 217–221.

Kawamura, K., M. Kobayashi, N. Tsubonuma, M. Mochida, T. Watanabe, and M. Lee (2004), Organic and inorganic compositions of marine aerosols from East Asia: Seasonal variations of water soluble dicarboxylic acids, major ions, total carbon and nitrogen, and stable C and N isotopic composition, in *Geochemical Investigation in Earth and Space Science; A Tribute to Issac R. Kaplan*, *Publication Series No. 9*, edited by R. J. Hill et al., pp. 243–265, The Geochemical Society, Elsevier.

Kim, Y.-P., and J. H. Seinfeld (1995), Atmospheric gas-aerosol equilibrium: III. Thermodynamics of crustal elements Ca^{2+}, K^+, and Mg^{2+}, *Aerosol Sci. Technol.*, *22*, 93–110.

Kim, Y. P., S.-G. Shim, K. C. Moon, C.-G. Hu, C. H. Kang, and K. Y. Park (1998), Monitoring of air pollutants at Kosan, Cheju Island, Korea, during March–April 1994, *J. Appl. Meteorol.*, *37*, 1117–1126.

Kundu, S., K. Kawamura, T. W. Andreae, A. Hoffer, and M. O. Andreae (2010), Diurnal variation in the water-soluble inorganic ions, organic carbon and isotopic compositions of total carbon and nitrogen in biomass burning aerosols from the LBA-SMOCC campaign in Rondônia, Brazil, *J. Aerosol. Sci.*, *41*, 118–133.

Lee, M., M. Song, K. J. Moon, J. S. Han, G. Lee, and K.-R. Kim (2007), Origins and chemical characteristics of fine aerosols during the northeastern Asia regional experiment (Atmospheric Brown Cloud-East Asia Regional Experiment 2005), *J. Geophys. Res.*, *112*, D22S29, doi:10.1029/2006JD008210.

Li, J., Z. Wang, H. Akimoto, C. Gao, P. Pochanart, and X. Wang (2007), Modeling study of ozone seasonal cycle in lower troposphere over east Asia, *J. Geophys. Res.*, *112*, D22S25, doi:10.1029/2006JD008209.

Mariotti, A., J. C. Germon, and A. Leclerc (1982), Nitrogen isotope fractionation associated with the NO_2^- to N_2O step of denitrification in soils, *Can. J. Soil Sci.*, *62*, 227–241.

Mariotti, A., C. Lancelot, and G. Billen (1984), Natural isotopic composition of nitrogen as a tracer of origin for suspended organic matter in the Scheldt estuary, *Geochim. Cosmochim. Acta*, *48*, 549–555.

Marsh, A. W. (1978), Sulphur and nitrogen contribution to the acidity of rain, *Atmos. Environ.*, *12*, 401–406.

Martinelli, L. A., P. B. Camargo, L. B. L. S. Lara, R. L. Victoria, and P. Artaxo (2002), Stable carbon and nitrogen isotopic composition of bulk aerosol particles in a C4 plant landscape of southeast Brazil, *Atmos. Environ.*, *36*(14), 2427–2432.

McMurray, P. H. (2000), A review of atmospheric aerosol measurements, *Atmos. Environ.*, *34*, 1959–1999.

Meng, Z., and J. H. Seinfeld (1996), Time scales to achieve atmospheric gas-aerosol equilibrium for volatile species, *Atmos. Environ.*, *30*, 2889–2900.

Moore, H. (1974), Isotopic measurement of atmospheric nitrogen compounds, *Tellus*, *26*, 169–174.

Moore, H. (1977), The isotopic composition of ammonia, nitrogen dioxide and nitrate in the atmosphere, *Atmos. Environ.*, *11*, 1239–1243.

Morin, S., J. Savarino, M. M. Frey, F. Domine, H.-W. Jacobi, L. Kaleschke, and J. M. F. Martins (2009), Comprehensive isotopic composition of atmospheric nitrate in the Atlantic Ocean boundary layer from 65°S to 79°N, *J. Geophys. Res.*, *114*, D05303, doi:10.1029/2008JD010696.

Ottley, C. J., and R. M. Harrison (1992), The spatial distribution and particle size of some inorganic nitrogen species over the North Sea, *Atmos. Environ.*, *26A*, 1689–1699.

Pakkanen, T. A. (1996), Study of formation of coarse particle nitrate aerosol, *Atmos. Environ.*, *30*, 2475–2482.

Park, M. N., Y. P. Kim, C.-H. Kang, and S.-G. Shim (2004), Aerosol composition change between 1992 and 2002 at Gosan, Korea, *J. Geophys. Res.*, *109*, D19S13, doi:10.1029/2003JD004110.

Pichlmayer, F., W. Schöner, P. Seibert, W. Stichler, and D. Wagenbach (1998), Stable isotope analysis for characterization of pollutants at high elevation alpine sites, *Atmos. Environ.*, *32*, 4075–4085.

Richter, A., J. P. Burrows, H. Nüß, C. Granier, and U. Niemeier (2005), Increase in tropospheric nitrogen dioxide over China observed from space, *Nature*, *437*, 129–132, doi:10.1038/nature04092.

Russell, K. M., J. N. Galloway, S. A. Macko, J. L. Moddy, and J. R. Scudlark (1998), Sources of nitrogen in wet deposition to the Chesapeake Bay region, *Atmos. Environ.*, *32*, 2453–2465.

Savarino, J., J. Kaiser, S. Morin, D. M. Sigman, and M. H. Thiemens (2007), Nitrogen and oxygen isotopic constraints on the origin of atmospheric nitrate in coastal Antarctica, *Atmos. Chem. Phys.*, *7*, 1925–1945.

Spokes, L. J., S. G. Yeatman, S. E. Cornell, and T. D. Jickells (2000), Nitrogen deposition to the eastern Atlantic Ocean, The importance of south-easterly flow, *Tellus*, *52B*, 37–49.

Turekian, V. C., S. Macko, S. D. Ballentine, R. J. Swap, and M. Garstang (1998), Causes of bulk carbon and nitrogen isotope fractionations in the products of vegetation burns: laboratory studies, *Chem. Geol.*, *152*, 181–192.

Vogel, J. C., A. S. Talma, and T. H. E. Heaton (1981), Gaseous nitrogen as evidence for denitrification in ground water, *J. Hydrol.*, *50*, 191–200.

Wagenbach, D., M. Legrand, H. Fischer, F. Pichlmayer, and E. W. Wolff (1998), Atmospheric near-surface nitrate at coastal Antractic sites, *J. Geophys. Res.*, *103*, 11,007–11,020, doi:10.1029/97JD03364.

Wall, S. M., W. John, and J. L. Ondo (1988), Measurement of aerosol size distributions for nitrate and major ionic species, *Atmos. Environ.*, *22*, 1649–1656.

Wang, G., K. Kawamura, M. Xie, S. Hu, J. Cao, Z. An, J. G. Waston, and J. C. Chow (2009), Organic molecular compositions and size distributions of Chinese summer and autumn aerosols from Nanjing: Characteristic haze event caused by wheat straw burning, *Environ. Sci. Technol.*, *43*, 6493–6499.

Widory, D. (2007), Nitrogen isotopes: Tracers of origin and processes affecting PM_{10} in the atmosphere of Paris, *Atmos. Environ.*, *41*, 2382–2390.

Wolff, G. T. (1984), On the nature of nitrate in coarse continental aerosols, *Atmos. Environ.*, *18*, 977–981.

Xiao, H.-Y., and C.-Q. Liu (2002), Sources of nitrogen and sulfur in wet deposition at Guiyang, southwest China, *Atmos. Environ.*, *36*(33), 5121–5130.

Yeatman, S. G., L. J. Spokes, and T. D. Jickells (2001a), Comparisons of coarse-mode aerosol nitrate and ammonium at two polluted coastal sites, *Atmos. Environ.*, *35*, 1321–1335.

Yeatman, S. G., L. J. Spokes, P. F. Dennis, and T. D. Jickells (2001b), Comparisons of aerosol nitrogen isotopic composition at two polluted coastal sites, *Atmos. Environ.*, *35*, 1307–1320.

Yeatman, S. G., L. J. Spokes, P. F. Dennis, and T. D. Jickells (2001c), Can the study of nitrogen isotopic composition in size-segregated aerosol nitrate and ammonium be used to investigate atmospheric processing mechanism?, *Atmos. Environ.*, *35*, 1337–1345.

Zhang, X., and P. H. McMurray (1992), Evaporative losses of fine particulate nitrates during sampling, *Atmos. Environ.*, *26A*, 3305–3312.

Zhuang, H., C. K. Chan, M. Fang, and A. S. Wexler (1999), Formation of nitrate and nonsea salt sulphate on coarse particles, *Atmos. Environ.*, *33*, 4223–4233.

K. Kawamura and S. Kundu, Institute of Low Temperature Science, Hokkaido University, Sapporo 060-0819, Japan. (kawamura@lowtem.hokudai.ac.jp)

M. Lee, Department of Earth and Environmental Sciences, Korea University, Seoul 136-701, South Korea.